Phytonanofabrication of magnetic iron oxide nanoparticles using *Cymbopogon citratus* and *Hylocereus undatus*: Application in the photocatalytic degradation of cationic dye

A DISSERTATION SUBMITTED

FOR THE PARTIAL FULFILLMENT OF THE DEGREE OF

MASTER OF SCIENCE

IN

CHEMISTRY

Submitted by:

URVASHI CHAWLA

2K22/MSCCHE/46

(ACADEMIC SESSION: 2023-24)

Under the supervision of

DR. POONAM SINGH

DEPARTMENT OF APPLIED CHEMISTRY

DELHI TECHNOLOGICAL UNIVERSITY

(Formerly Delhi College of Engineering)
BAWANA ROAD, ROHINI,
NEW DELHI-110042

MAY, 2024

CANDIDATE'S DECLARATION

I **Urvashi Chawla** (2K22/MSCCHE/46) student of M.Sc. (Applied Chemistry), hereby declare that the dissertation work entitled **"Phytonanofabrication of magnetic iron oxide nanoparticles using Cymbopogon citratus and Hylocereus undatus: Application in the photocatalytic degradation of cationic dye"** which is submitted by me to the Department of Applied Chemistry, Delhi Technological University in partial fulfillment of the award of degree of Masters of Science in Chemistry, is original and not copied from any source without proper citation. This work has not previously formed the basis for the award of any Degree, Diploma Associateship, Fellowship, or other similar title or recognition.

Place: Delhi

Date: 30 MAY 2024 **URVASHI CHAWLA**

DEPARTMENT OF APPLIED CHEMISTRY

DELHI TECHNOLOGICAL UNIVERSITY

(Formerly Delhi College of Engineering)

Bawana Road, Rohini, New Delhi-110042

CERTIFICATE

I hereby certify that the Project Dissertation titled **"Phytonanofabrication of magnetic iron oxide nanoparticles using Cymbopogon citratus and Hylocereus undatus: Application in the photocatalytic degradation of cationic dye"** which is submitted by **Urvashi Chawla** (2K22/MSCCHE/46), Department of Applied Chemistry, Delhi Technological University, Delhi, in partial fulfillment of the requirement for the award of the degree of Master of Science in Chemistry. This is the record of the project work carried out by her under my supervision. To the best of my knowledge, this work has not been submitted in part or full for any degree or diploma to this university or elsewhere.

Place: Delhi

DR. POONAM SINGH

SUPERVISOR

Date: 30 MAY 2024

ACKNOWLEDGEMENT

I firmly believe that academic achievements are strongly linked to the selection of a suitable mentor and advisor. I had the privilege of conducting my dissertation under the supervision of Dr. Poonam Singh, Assistant Professor in the Department of Applied Chemistry at Delhi Technological University. I express deep and sincere gratitude to her for unwavering support, valuable insights, and expert feedback throughout this process. I also appreciate the contributions of the faculty members in the Department of Applied Chemistry at Delhi Technological University for their guidance on my project thesis.

I am profoundly thankful to Prof. Prateek Sharma, the Vice Chancellor of Delhi Technological University, and Prof. Anil Kumar, the Head of the Department of Applied Chemistry, for granting permission to work within the department and providing the essential resources to ensure the successful project completion.

I express my heartfelt gratitude and regards to Jigyasa Pathak, Ph.D. Research Scholar of Department of Applied Chemistry, Delhi Technological University, for innumerable fruitful discussions and valuable assistance during this research work.

I wish to acknowledge the contributions of other Research Scholars, Dr. Bhamini Pandey, Priyanka Yadav and Sarla Yadav. I am grateful for the support of my classmates, Ankit, Rizwan, Indu and Manju.

Finally, I am deeply appreciative of my family's steadfast support and motivation during this scholarly endeavour. Additionally, I am thankful to God for granting me with the strength to persevere.

URVASHI CHAWLA

ABSTRACT

This dissertation explores an eco-friendly way of synthesizing magnetic iron oxide nanoparticles using lemon grass (*Cymbopogon citratus*) leaf and dragon fruit (*Hylocereus undatus*) peel extract. To analyse iron oxide nanoparticles formation, characterization techniques were performed such as X-ray Diffraction (XRD), Fourier Transform Infrared Spectroscopy (FTIR), Scanning Electron Microscopy (SEM) with Energy Dispersive X-Ray Analysis (EDX), Vibrating-sample Magnetometry (VSM) and Zeta Potential measurements. The sample prepared using lemon grass extract was exposed to UV light and used as a photocatalyst for the decomposition of methylene blue (MB) dye. This photocatalyst under light exposure displayed a significant capability, as these nanoparticles decomposed 93% of MB dye within a span of 120 minutes. The phytonanofabrication of iron oxide nanoparticles has potential as photocatalyst in degrading textile dye for dye removal as wastewater remediation.

TABLE OF CONTENTS

LIST OF FIGURES

Figure 17: Zeta potential plot of iron oxide nanoparticles synthesized using (a) lemon grass leaf extract and (b) dragon fruit peel extract.

Figure 18: Room temperature MH curve for the of iron oxide nanoparticles prepared using lemon grass leaf extract.

Figure 19: Room temperature MH curve for the of iron oxide nanoparticles prepared using dragon fruit peel extract.

Figure 20: UV-visible spectroscopy analysis of green synthesized iron oxide nanoparticles prepared using lemon grass leaf extract representing photocatalytic MB dye decomposition activity.

Figure 21: Photocatalytic proposed mechanism of iron oxide photocatalyst.

LIST OF TABLES

LIST OF ABBREVIATIONS

IO	iron oxide
NPs	nanoparticles
L	Lemon grass
D	Dragon fruit
C. citratus	*Cymbopogon citratus*
H. undatus	*Hylocereus undatus*
BOD	Biochemical Oxygen Demand
COD	Chemical Oxygen Demand
UV	Ultraviolet
mV	Milli volt
mg/L	Milli gram/ Litre
kOe	Kilo Oersted
min	minutes
pH	potential of hydrogen
nm	nanometer
rpm	revolution per minute

Chapter 1 Introduction and Literature Survey

1.1 Remediation of wastewater

The global challenge of sustainable water resource management is multifaceted and urgent, requiring comprehensive strategies to tackle supply and quality issues. One of the most pressing concerns is water pollution, mainly caused by residential and industrial wastewater **(Yohannes Getahun 2022)**. Water contamination is influenced by multiple factors such as marine dumping, industrial discharges, insufficient sewage treatment, radioactive waste, and agricultural runoff **(Asim Ali Yaqoob 2020)**. Over the years, the release of inadequately treated wastewater into water bodies has emerged as significant environmental problem. This concern has been exacerbated since the Industrial Revolution, a period marked by swift rise in industrial activities and urbanization. Industries such as the textile sector have notably contributed substantially to water pollution during this era **(Bhamini Pandey 2021) (Jayaraj Iyyappan 2024).**

The textile manufacturing sector has been a prime culprit in releasing a variety of pollutants into water ecosystems. This industry frequently relies on the use of coloured additives, including dyes and pigments, introducing organic contaminants into the environment. These dyes are not only aesthetically disturbing in waterways but also pose serious environmental and health risks **(Muhammad Noman 2020)**. Organic contaminants found in dyes can be highly toxic, mutagenic (potential to alter genetic material), and carcinogenic (cancer causing). The release of these substances into the environment can have detrimental health consequences for humans. For example, contact with polluted water might lead to skin allergies, acute toxicity, and long-term health problems such as affect the central nervous system and risk of developing various forms of cancer **(Alex Mbachu 2023) (Muhammad Farooque Lanjwani 2024)**. The ecological repercussions of these pollutants are equally concerning. Organic toxins present in dyes can severely disrupt the balance of aquatic ecosystems. One major environmental consequence is the diminished penetration of sunlight in water bodies, impeding the process of photosynthesis. This process is crucial for the survival of aquatic plants and the vitality of entire water-based ecosystems. When

photosynthesis is inhibited, it can lead to the decline of oxygen-generating plants, thereby affecting the entire aquatic food chain **(Sohini Dutta 2024)**.

Additionally, the presence of organic pollutants in marine environment increases the biochemical oxygen demand (BOD) and chemical oxygen demand (COD). BOD measures the oxygen necessary for aerobic biological organisms to decompose organic matter in water, whereas COD determines the oxygen required to oxidize both organic and inorganic substances chemically. Elevated BOD and COD levels indicate that considerable oxygen is being consumed to break down pollutants, potentially leading to reduced oxygen levels in water bodies. This oxygen depletion, also referred as hypoxia, can create dead zones for aquatic life, thus endangering biodiversity and the equilibrium of aquatic ecosystems **(Hisham A. Maddah 2022).**

In order to address these challenges that affect both biotic and abiotic segments of environment, a variety of conventional and modern methods have been inspected for purification of wastewater to attain efficient solutions. These methods encompass a spectrum from physical processes like sedimentation and filtration to biological operations such as activated sludge and biofilm-based reactors, and chemical strategies including coagulation, flocculation, and advanced oxidation processes (AOPs). However, these techniques have its own advantages and disadvantages in order to ensure long-term sustainability, dependability, and affordability **(Meerambika Behera 2021) (Sarkodie 2023).** In the range of chemical strategies, there is addition of chemicals to precipitate, oxidize, or reduce contaminants. Coagulation and flocculation are widely practiced techniques where chemicals like alum or ferric chloride are added to clump and settle suspended particles. Nonetheless, these processes often result in the production of significant amounts of sludge that require proper disposal. Advanced oxidation processes (AOPs) are ecological that have gained prominence in this category of wastewater treatment due to their ability to degrade numerous pollutants with less toxicity **(Virendra K. Saharan 2014) (Chandrakant R. Holkar 2016)**.

In scholarly literature, the prevailing classification of Advanced Oxidation Processes (AOPs) into the following categories: (a) UV–hydrogen peroxide (b) Fenton and photo-Fenton

reactions (c) Ozone-based (d) Photocatalysis and (e) Sonolysis. These categories represent distinct methods for treating wastewater, each leveraging specific mechanisms to promote oxidation and breakdown of containments **(Yang Deng 2015) (Pavlos K. Pandis 2022)**. Photocatalytic water treatment has recently garnered considerable attention due to its distinct advantages over other AOPs. This method is favoured because it operates efficiently under normal pressure and temperature conditions, incurs low costs and avoids the generation of secondary waste. Its impressive performance and environmentally friendly nature make the process as a modern and sustainable technology for wastewater decontamination **(Marwah A. Al-Nuaim 2023)**.

1.2 Photocatalysis

Photocatalysis is performed by harnessing light energy to generate reactive oxygen forms include superoxide ($^{\bullet}O_2^-$) and hydroxyl ($^{\bullet}OH$) radicals in order to break down pollutants efficiently. This method involves a catalyst, often a semiconductor like titanium dioxide (TiO_2) as a prominent example, which absorbs light under standard temperature and pressure conditions **(Debika Devi Thongam 2021).** When exposed to light, typically UV or visible, electrons are promoted in the catalyst from the valence band to the conduction band, resulting in the formation of positive holes. These electrons and holes move towards the catalyst surface engaging in redox reactions that result in the breakdown of pollutants **(Nafees Ahmad 2021)**. Photocatalysis combines "photo," meaning light, with "catalysis," which accelerates a chemical reaction without being used up in the method. Photocatalysis was introduced in 1972 when Fuji, Sharma, and Honda observed water splitting under ultraviolet (UV) light. Since then, research in this area has grown rapidly due to its wide-ranging potential and practical applications **(Mohammad Mansoob Khan 2023).**

There are two main types of photocatalysis: homogeneous and heterogeneous. In homogeneous, the photocatalyst and reactants are in the same phase, typically dissolved in a solvent. On the other hand, heterogeneous photocatalysis involves the photocatalyst and reactants being in different phases, typically with the catalyst as a solid form and reactants

as liquid or gas phases **(Mohammad Mansoob Khan 2023)**. Figure 1 represent the general mechanism of photocatalytic process including chemical reactions.

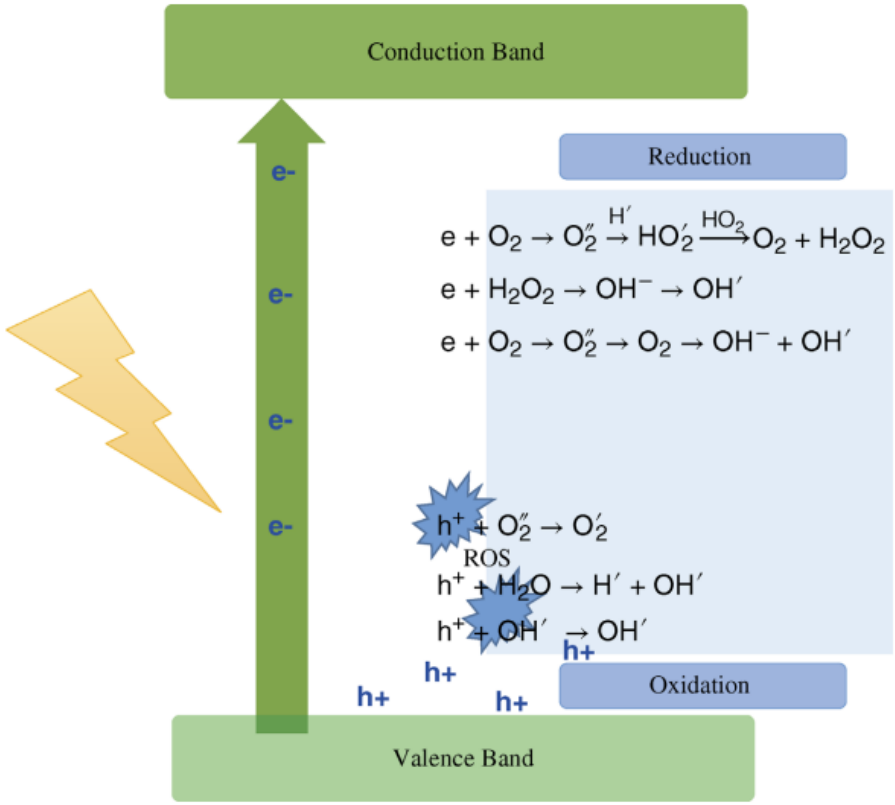

Figure 1: Mechanism of photocatalytic process including chemical reactions **(Azad Qayoom Malik 2022)**.

In recent years, the integration of nanomaterials has significantly enhanced the field of photocatalysis. Nanoparticles, nanotubes, nanowires, porous nanospheres, and nanorods are examples of nanomaterials that offer a high surface area and large surface energy, resulting in improvement in terms of reactivity **(Muhammad Bilal Tahira 2020)**. These nanostructured materials possess unique properties that surpass those of their bulk counterparts. Apart from acting as adsorbents, various nanomaterials demonstrate exceptional photocatalytic performance, effectively degrading dyes and organic substances. This marks a major breakthrough in environmental remediation technologies due to incorporation of nanomaterials into photocatalysis **(Richa Tomar 2020)**.

1.3 Nanomaterials in wastewater treatment

The worldwide issue of water contamination and persistent need for fresh water necessitates the exploration of cutting-edge technologies for purifying water. Scientists are continually striving to develop new, affordable methods to improve water treatment efficiency **(Arunachalam Thirunavukkarasu 2020)**. Nanotechnology represents a promising and rapidly advancing field in various domains like medicine, healthcare, electronics, information technology, energy and environment. The use of nanomaterials is gaining recognition to tackle environmental concerns such as wastewater remediation due to their intriguing properties **(Sasan Zahmatkesh 2023)**.

The National Nanotechnology Initiative (NNI) defines nanomaterials as materials sized between 1 and 100 nanometers (nm). Nanomaterials possess distinct attributes such as nano scale, expanded surface area, robust reactivity, mechanical strength, porosity, hydrophilicity, dispersibility, and hydrophobicity enhancing their efficacy for purifying wastewater **(Hamidreza Sadegh 2017) (Bapun Barik 2020)**. These unique properties enable them to efficiently eliminate a broad spectrum of contaminants including heavy metals such as lead (Pb) and molybdenum (Mo), along with a variety of organic and inorganic impurities as well as harmful microorganisms **(Haleema Saleem 2020)**.

In the past twenty years, significant progress has been achieved in the development of innovative nanomaterials for a variety of wastewater treatment applications. This encompasses the exploration of fresh materials, the establishment of simple, eco-friendly, economical production processes, and synthesis of nanocomposite materials. Different types of nanomaterials have been applied in wastewater purification, demonstrating their adaptability and efficiency in dealing with different pollutants **(N. A. Ahmad 2021)**. Recent advancements have led to the evolution of nanoparticle-based photocatalysts, nano-sized motors, ultra-thin membranes, and nanosorbents. Nanophotocatalysts enhance the reactivity of catalysts by virtue of their large surface area and shape-dependent characteristics which improve their electrical, mechanical, magnetic, chemical reactivity as well as optical properties. These nanoparticles can facilitate oxidation reactions by effectively generating

oxidizing species on their surfaces to aid in pollutant degradation **(Asim Ali Yaqoob 2020) (Wajid Umar 2022)**.

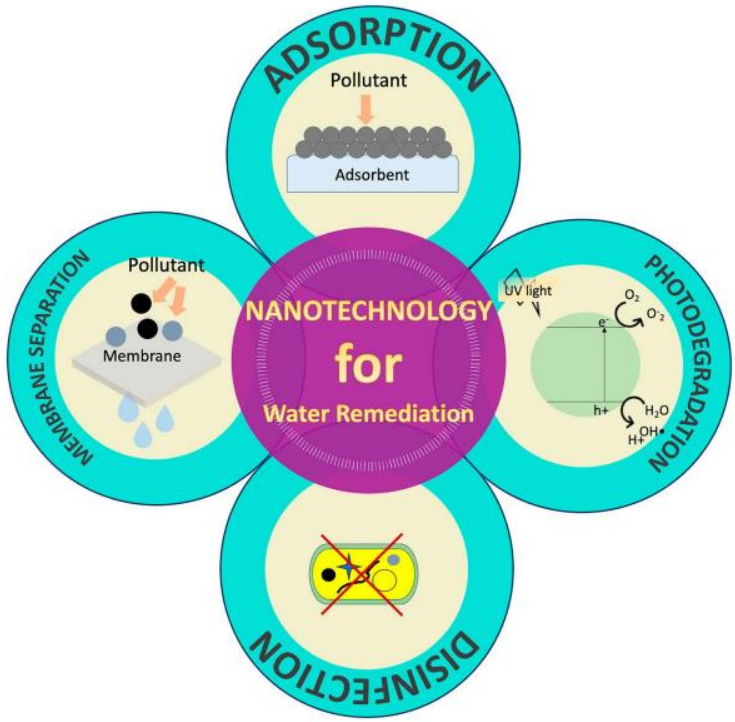

Figure 2: Illustration of the roles and applications of nanomaterials for water remediation **(N. A. Ahmad 2021)**.

To determine the most suitable approach and substance for treating wastewater is a remarkably intricate task, requiring consideration of factors such as standards of quality, efficiency, and expenses. Therefore, it is crucial to take into account treatment flexibility and effectiveness, reuse of treatment materials, environmental safety and sustainability, as well as affordability **(xu 2012).** In the literature, researchers have reported numerous kinds of nanomaterials used in wastewater treatment. These include metal-based nanoparticles, polymer nanoparticles, zeolites, carbon-based nanomaterials, self-assembled monolayers on mesoporous supports (SAMMS), biopolymers, and nanoscale metal oxide and chalcogenide semiconductor photocatalysts **(Lavanya Madhura 2018)**. Within these, titanium dioxide (TiO_2), zinc oxide (ZnO), iron oxide (Fe_2O_3/Fe_3O_4), and cerium oxide (CeO_2) are

particularly notable metal oxide nanoparticles due to their high reactivity and photolytic properties. Their exceptional ability to adsorb various pollutants in water and wastewater is attributed to their distinct characteristics, such as strong reactivity, selectivity, extensive surface area, and significant functionalization **(Tadele Assefa Aragaw 2021).**

Magnetic nanoparticles (MNPs) are a notable form of nanomaterials that have been widely recognized as a useful tool for wastewater remediation. The utilization of MNPs in treating wastewater holds significant potential for achieving greater efficiency of filtration materials, advancing reuse and recycling efforts along with minimizing energy consumption **(Jenifer Gómez-Pastora 2017)**. Application of nano remediation with magnetic nanomaterials has the capacity to lower overall costs, treatment duration, and facilitate *in-situ* treatment, approaching near-perfect efficiency **(Saurabh Shukla 2021).**

Within the magnetic nanoparticles, zero-valent iron and iron oxide nanoparticles, are considered highly effective for adsorbing and removing pollutants from wastewater. These nanoparticles are promising candidates as they offer cost-effectiveness, high adsorption capabilities, easy separability, and improved stability for large-scale industrial wastewater treatment. The efficacy of iron oxide nanomaterials in removing pollutants have been demonstrated by both laboratory and field-scale trials **(Rachna Bhateria 2019) (Basem E. Keshta 2024)**.

1.3.1 Iron Oxide Nanoparticles

Iron oxides exist in variety of pure phases, including oxides, hydroxides, and oxyhydroxides. These types include $Fe(OH)_3$, $Fe(OH)_2$, $Fe_5HO_8{\cdot}4H_2O$, Fe_3O_4, FeO as well as five polymorphs of FeOOH, and four variations of Fe_2O_3. Hematite (α-Fe_2O_3), Magnetite (Fe_3O_4), and Maghemite (γ-Fe_2O_3) are the most important types in terms of technological perspective **(Jiří Tuček 2015) (Attarad Ali 2016)**.

Magnetite, commonly referred to as black iron oxide, possesses an inverse spinel configuration where Fe^{3+} ions are dispersed arbitrarily among octahedral and tetrahedral sites, while Fe^{2+} ions occupy octahedral sites **(Teja 2009)**. This particular structure

contributes to the strong magnetic characteristics of magnetite, rendering it valuable in applications like magnetic storage devices, MRI, and its use as a magnetic adsorbent in water treatment. Additionally, depending on its composition and method of synthesis, magnetite can function as both an n-type and p-type semiconductor **(Christianna N. Lininger 2018)**.

Maghemite has a cubic structure, resembling magnetite but containing vacancies in the cation sublattice. As nanoparticles less than 15 nm, this form displays ferrimagnetic properties and demonstrates superparamagnetic behaviour. Maghemite is metastable and has the ability to convert into hematite under heat exposure. Its notable magnetic response and compatibility with biological systems making it viable option for biomedical uses, including as MRI contrast agents and components of drug delivery systems **(Rachna Bhateria 2019)**.

Hematite, also referred to as ferric oxide is the steady type of iron oxide and is commonly present in rocks and soils. It is also identified as red ochre, specularite, and martite **(Teja 2009)**. It has a hexagonal close-packed structure with Fe^{3+} ions filling two-thirds of the octahedral sites. Functioning as an n-type semiconductor with a bandgap energy of approximately 2.1 electrovolts enables its utility in gas sensors, pigments, and catalysts. It is also recognized as exceptional corrosion resistance and the final product resulting from the transformation of other iron oxides **(Rachna Bhateria 2019)**. The positioning of the (1102) plane in the trigonal and hexagonal unit cells of α-Fe2O3, which possesses the corundum structure. The dimensions of the α-Fe2O3 unit cell are a = b = 5.04 Å and c = 13.77 Å. The basal plane of oxygen is situated within the, or c-cut plane. There is no overall dipole moment in the repeating unit perpendicular to the surface, making α- Fe2O3(1102) a non-polar surface **(Florian Kraushofer 2017).**

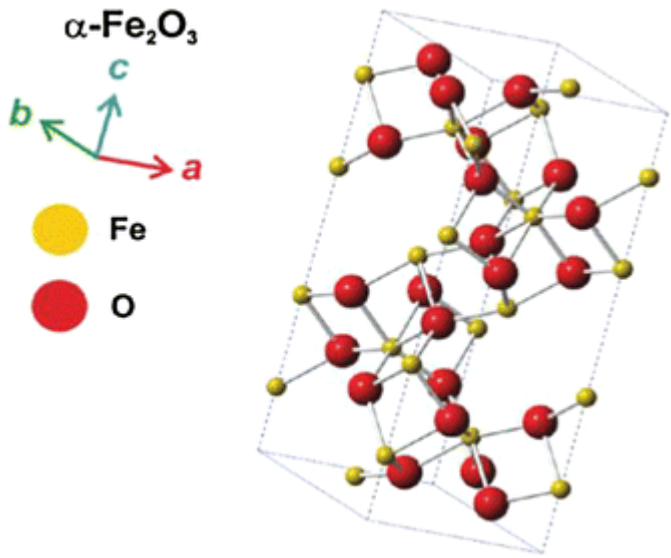

Figure 3: α-Fe_2O_3 crystal structure **(A. Mirzaei 2016).**

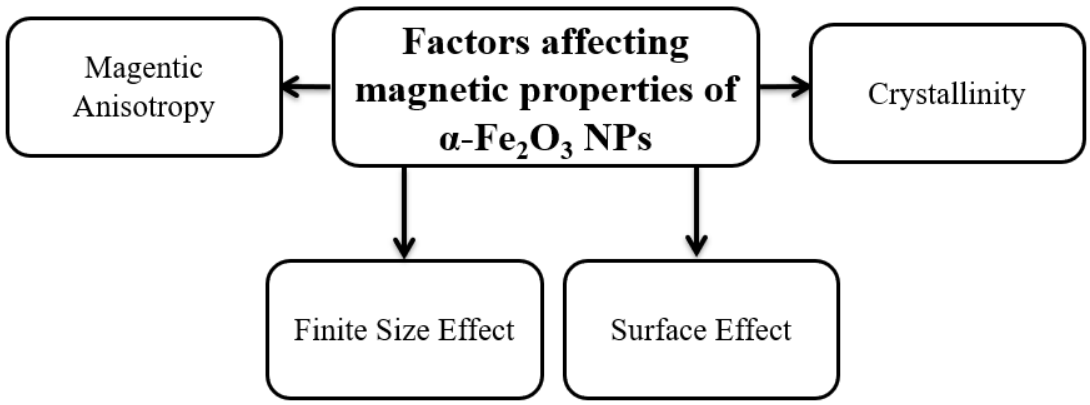

Figure 4: Factors affecting magnetic properties of α-Fe_2O_3 nanoparticles

These nanoparticles are weakly ferromagnetic or antiferromagnetic depending on the temperature antiferromagnetic order below their Néel temperature (955 K) and possess a corundum crystal structure. There are various factors affecting magnetic properties of α-Fe_2O_3 nanoparticles represented by Figure 4 **(Alec P. LaGrow 2013) (Bashar Issa 2013).** Hematite nanoparticles are used in various applications including gas sensors, pigments, catalysts, and as a precursor for synthesizing other iron oxides like magnetite and maghemite

(Haibo Guo 2012). Their n-type semiconducting properties and high corrosion resistance make them suitable for diverse technical and biomedical applications. Furthermore, the band gap of 2.1 eV allows for applications in electronics and photovoltaics **(Rachna Bhateria 2019)**. In conclusion, iron oxide nanoparticles, especially α-Fe2O3, have significant potential in variety of applications specially wastewater remediation through photocatalysis owing to their distinctive physical and chemical characteristics.

1.4 Green synthesis of iron oxide nanoparticles

Top-down and bottom-up strategies are frequently employed in the synthesis of nanomaterials as represented in Figure 5. The top-down approach involves the reduction of bulk materials into fine particles through lithographic methods like grinding, laser ablation, thermal ablation, and milling. In contrast, the bottom-up relies on chemical and biological techniques to assemble atoms, molecules, and smaller particles to create nanoparticles **(Singh J 2018) (Md Ishak 2019)**. Despite their efficacy, conventional synthesis methods for transition metal oxides (TMOs) have drawbacks such as expensive operational costs, substantial energy input requirements, reliance on hazardous precursors, and the production of toxic by-products **(Jigyasa Pathak 2023)**.

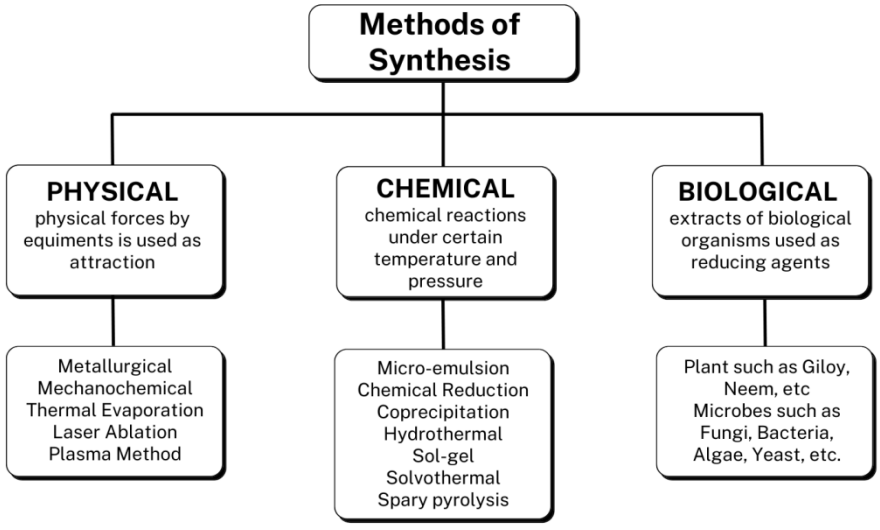

Figure 5: Conventional method of production of iron oxide nanoparticles.

Considering the challenges posed by environmental concerns and economic constraints, there is a strong need to implement biosynthesis processes for producing nanoparticles. It has resulted in the development of simple, sustainable, environmentally-friendly, and cost-efficient methods guided by twelve green principles **(Jeevanandam 2022)**. The bio fabrication of nanomaterials encompasses various biological agents like plants, bacteria, fungi, algae etc. Preferably, phyto-nanotechnology has gained global attention due to the abundant biomass from many species, presence of effective plant chemicals and biodegradability. Lately, nanoparticles have been created using diverse plant-derived extracts due to wide-ranging applications across fields such as biomedicine, electronics, cosmetics, and agriculture **(Mohamed A 2020) (Sharma R 2022)**.

Plant-assisted synthesis is an efficient method to boost the effectiveness of phytochemicals, eliminate toxicity, and offer promising applications as nanoparticles. In green synthesis, water serves as the primary solvent, along with non-toxic and environmentally friendly chemicals **(Castro-Puyana 2017)**. The use of plants for nanoparticle biosynthesis presents several advantages over bacteria, fungi, algae, and other biological organisms. This includes cost-effectiveness and ease of extraction compared to traditional methods, presence of various metabolites favouring kinetic routes over alternative methods, and lower maintenance requirements in comparison to preserving microbial cultures **(Asmaa Mohamed El Shafey 2020)**. The extracts from leaves, stems, fruits, flowers pulp seeds and other plant parts act as agents for reduction, capping biomolecules and controlling ions into atoms that have functional group for stabilization. The active sources convert precursor elements into ions, then transition into atoms as a bottom-up process resulting in growth of nanoparticles housing functional group capping biomolecules **(Priya 2021) (Jabbar 2022)**.

This study investigates the biosynthesis of iron oxide nanoparticles by employing two different extracts such as lemongrass (*C. citratus*) leaf extract and dragon fruit (*H. undatus*) peel extract as reducing and capping agents. The synthesized nanoparticles were characterized using X-ray diffraction (XRD), Scanning electron microscope (SEM), Fourier-transform infrared spectroscopy (FTIR), Zeta Potential and Vibrating sample magnetometer (VSM) to evaluate the structural morphology. Moreover, the research examines the

photocatalytic efficiency of these nanoparticles in degrading textile dye for dye removal as wastewater remediation.

1.5 Lemon grass (*Cymbopogon citratus*) and Dragon fruit (*Hylocereus undatus*)

Cymbopogon citratus (C. citratus), a plant commonly referred to as lemon grass, is a tall and quickly growing perennial grass with lemon-scented leaves rich in volatile oils. It belongs to the Poaceae (Gramineae) family and generally grows in tropical and semi-tropical regions across Asia, Africa, Central, and South America. It contains diverse bioactive compounds like phenols, flavonoids, saponins, aldehydes, alcohols and esters that contribute to antibacterial, antioxidant, antifungal and anticarcinogenic properties **(Lawal 2017)**. Therefore, *C. citratus* is a natural alternative for the reducing metal oxide precursors, aiding in production, stabilization, and functionalization of the iron oxide nanoparticles.

Table 1: Primary and secondary metabolites of Lemon Grass and Dragon Fruit.

Lemon Grass (*C. citratus*)	**Dragon Fruit (*H. undatus*)**
Flavonoids	Flavonoids
Phenol	Steroids
Saponins	Pectin
Terpenes	Triterpenoids
Alkaloids	Alkaloids

Dragon fruit, also known as Pitaya, is a perennial mounting cactus that belongs to the Cactaceae family and the Hylocereus genus. This fruit comes in three main varities: *Hylocereus undatus* (white pulp with red peel), *Selenicereus megalathus* (white pulp with yellow peel), and *Hylocereus polyrhizus* (red pulp with red peel). *H. undatus* is particularly notable for its red exterior with green fins and is affluent in antioxidants, vitamins, and minerals that may assist intercepting various diseases, including cancer, cardiovascular

issues, diabetes, gastrointestinal problems, respiratory illnesses, and urinary conditions **(Mustafa Taha Mohammed 2019)**. The peel of the dragon fruit contains several beneficial compounds, such as pectin, phyllocactin, betanin, triterpenoids, betacyanin, and steroids. These compounds have significant pharmacological activities, including antimicrobial, antioxidant, anti-tumor, and anti-inflammatory properties. Moreover, the non-edible portions of the fruit are being explored as potential cost-effective sources of enriched products, especially given the significant amount of fruit waste generated by the food industry during juice production **(S. Shyamalagowri 2022)**.

1.6 Conclusion

Water pollution remains a critical global concern, particularly due to industrial discharges containing toxic dyes. To combat this, advanced oxidation processes (AOPs) like photocatalysis, enhanced by nanomaterials play a vital role in wastewater treatment. Green synthesis methods for metal oxides and magnetic nanoparticles utilizing plant-based materials to provide environmentally friendly alternatives to conventional production. Lemongrass possesses both antibacterial and antioxidant properties, while dragon fruit is abundant in beneficial compounds to act as efficient reducing agents for the production of magnetic iron oxide nanoparticles.

The novelty aspect of this research lies in the use of lemongrass leaf extract to synthesize magnetic iron oxide nanoparticles, which are then uniquely employed for photocatalysis in treating wastewater. Moreover, this study is pioneering in utilizing dragon fruit peels to produce magnetic iron oxide nanoparticles with potential application in photocatalytic water treatment. This combined method not only investigates novel biological resources for nanoparticle production but also demonstrates their efficiency in addressing wastewater remediation.

Chapter 2 Characterization Techniques

2.1 X-ray Diffraction (XRD)

The fundamental principle of X-Ray Diffraction (XRD) is the concept of constructive interference representing monochromatic X-rays diffracted from the sample. According to Bragg's Law ($2d\sin\theta = n\lambda$), constructive interference occurs when the path difference between reflected waves is an integer multiple of the wavelength **(Atkins E 1978)**.

XRD data may provide a variety of details, including the kind of phase present, preferred crystal growth direction, grain size, lattice parameters, the crystallinity of the material, etc. The Deby-Scherrer formula can be used to calculate average grain size **(Suryanarayana C 1998)**.

$$D\ (nm) = \frac{K\lambda}{\beta \cos\theta}$$

Where K = 0.94, β represent full width at half maximum (FWHM) in radians. XRD measurements were done by using Rigaku Miniflex II in the 2θ range of 20-80° in step-scanning mode, available at the Advanced Instrumentation Research Facility, Jawarharlal Nehru University (JNU), New Delhi.

Figure 6: Rigaku Miniflex II X-Ray Diffractometer

2.2 Scanning Electron Microscopy (SEM) with Energy Dispersive X-Ray Analysis (EDX)

Scanning electron microscopy (SEM) is an imaging method that generates high-resolution topographical and structural images, displaying either cross-sectional or plan-view perspectives of the sample. High-energy electron beams and atoms present in samples interact in many possible ways. These electrons emit particles (e.g. photons, electrons, etc.) from samples rather than transmitting through them and detected in the form of signals **(Parry KDV (2000)**. The signals are converted to visual signals shown on a cathode ray tube (CRT). This is one of the versatile instruments used for the examination and analysis of microstructural morphology and characterizations of chemical composition **(Zhou W 2007).**

Energy dispersive X-ray (EDX) analysis is a method for quantitatively analyzing elements using the characteristic spectrum of the interaction between electron beam and sample can produce X-rays, which occur when electrons from higher energy shells fill vacancies in the inner shell of atoms, causing emission of secondary electrons. EDX data can be used to determine the composition of a material **(Wei 2009).**

SEM images were acquired using a Zeiss Supra 55 Scanning Electron Microscope with high performance at variable pressure with integration of EDX analysis, available at the Centre for Nanoscience and Nanotechnology, Jamia Milia Islamia, New Delhi.

Figure 7: Zeiss Supra 55 Scanning Electron Microscope.

2.3 Fourier-Transform Infrared Spectroscopy (FTIR)

FTIR spectroscopy is an analytical technique that measures the absorption and emission of infrared radiation of the given sample. The primary objective is to measure the quantity of light that the sample absorbs, so that in depth study regarding the various functional groups, type of chemical bonding present in the sample can be established. There is one limitation in the conventional transmission mode of FTIR spectroscopy is that it possesses issue with the tissue penetration depth of IR signals, and can penetrate only up to certain micrometer length **(A. Fadlelmoula 2022).**

However, with new attachment in FTIR spectroscopy i.e. ATR-FTIR (Attenuated Total Reflectance), it has overcome the above limitation. It basically measures the reflected signals and thus able to analyse much thicker samples and higher absorbance samples for which conventional FTIR was not that efficient. Furthermore, it can be employed not only for the identification of organic compounds and functional groups within a sample, but also for pathological analysis. This technique enables the measurement of compositional changes in the sample, including chemical alterations, change in bonds, mass of molecules, etc. **(A. Fadlelmoula 2022).**

FT-IR spectrum was obtained from Department of Applied Physics of Delhi Technological University (DTU), New Delhi.

Figure 8: Perkin Elmer SPECTRUM BX II

2.4 Zeta Potential

Zeta potential, also referred to as electrokinetic potential, represents the electric potential difference that arises between the surface of a moving particle and the surrounding dispersing medium at the slipping plane **(Claure N. Lunardi 2020)**.

When the charged particles are dispersed in a given medium, on its surface ions/charges starts to accumulate and forms a double layer referred to as EDL. Inner layer inside the particle, consist of opposite charges to that on surface, called stern layer. Electrostatic effects diminish beyond the stern layer, in accordance with the Debye law. When this system is subjected to an external applied electric field, the charges within the diffuse layer move towards the opposite electrode, a phenomenon known as electrophoresis. Within the diffuse layer, there exists a hypothetical plane called slipping plane that serves as the interface between the particle and the surrounding fluid medium. It is the electrical potential measured at this interface **(Claure N. Lunardi 2020)**.

Zeta potential analysis was obtained from Department of Applied Chemistry of Delhi Technological University (DTU), New Delhi.

Figure 9: Zeta Potential Analyzer

2.5 Vibrating-sample magnetometry (VSM)

A Vibrating Sample Magnetometer, is an effective tool to measure the magnetic properties of material. Aim of this setup is to measure different magnetic moments in the magnetic sample as a function of external magnetic field and temperature. It can be used to study the nature of magnetization in the sample and strength of magnetic material. VSM is extensively used for magnetism study in diamagnetic, ferromagnetic, ferrimagnetic, antiferromagnetic and paramagnetic. VSM setup is based on the principle of electromagnetic induction, wherein moving part results in change in magnetic flux which produces the electric field, this change in the electric field produces the change in magnetic field. When a sample material is placed in the external magnetic field which is produced, dipole moments are being induced in the sample which is proportional to magnetic susceptibility and applied field. This moving part also generates sinusoidal waves which is proportional to magnetic moment, vibration amplitude and vibrational frequency **(B.R.Kirupakar 2016).**

VSM analysis were taken using Microsense ADE – EV9 available at University Science Instrumentation Center (USIC), University of Delhi, New Delhi.

Figure 10: Vibrating-sample magnetometry

2.6 Conclusion

This chapter summarizes the characterization techniques performed for the bio-synthesis of iron oxide nanoparticles using two different extracts. The synthesized samples were successfully characterized using XRD, SEM-EDX, Zeta potential, FTIR and VSM measurements.

Chapter 3 Synthesis of Iron Oxide Nanoparticles

3.1 Introduction

Iron is widely available elements on Earth and forms significant portion of the planet's crust. It plays a vital role in human society, being extensively utilized across various industries and applications. As a transition metal, iron has exceptional characteristics like multiple oxidation states and magnetic properties, which are further improved when it combines with oxides **(Dale L. Huber 2005)**. These attributes make iron oxides valuable in fields such as science and technology. Transition metal oxides, including iron oxides are highly intriguing to researchers due to their distinct physical, electrical, magnetic, and optical traits at the nanoscale level. These properties differ noticeably from their bulk counterparts because of factors such as high surface-to-volume ratio, and quantum confinement effects detected in nanoparticles **(Attarad Ali 2016) (Seyedeh-Masoumeh Taghizadeh 2020)**.

Iron oxide nanoparticles, with their widespread availability, low expense, environmental sustainability, and varied uses, have garnered significant interest. Extensive research has been conducted on iron oxide nanoparticles and they have found applications in fields like electronics, biomedical technology and environmental processes **(Wei Wu 2016)**. The current utilization of iron oxide nanomaterials in water treatment can be broadly classified categorized into two main approaches: influence to act as nanosorbents or carriers to improve removal efficiency, and those relying on their use as photocatalysts to degrade contaminants or convert them into less harmful forms **(Piao Xu 2012)**. IONPs possess distinct attributes such as biocompatibility, magnetic responsiveness and catalytic activity that make them favourable over other types of nanomaterials for numerous applications **(Alvaro Gallo-Cordova 2021).**

3.2 Synthesis of Iron Oxide Nanoparticles

Iron oxide nanoparticles has been synthesised using lemon grass leaf and dragon fruit peel extract under green approach.

3.2.1 Chemicals Required

Ferrous chloride tetrahydrate ($FeCl_2.4H_2O$), Ferric chloride anhydrous ($FeCl_3$), sodium hydroxide (NaOH), lemongrass (*Cymbopogon citratus*) leaves and dragon fruits (*Hylocereus undatus*) were collected from home garden and nearby market respectively, ethanol and distilled water were used as starting materials.

3.2.2 Preparation of *C. citratus* leaf extract

The lemongrass leaves were washed to remove the impurities and dried for 4 days under direct sunlight. The leaves were cut in small pieces, 10 g was added to a beaker along with 400 ml of distilled water. The beaker was covered and left at room temperature overnight. The beaker was then heated on a hot plate and boiled for about 4 hours, maintaining a temperature between 80-90 °C using a thermometer. The brownish-yellow colored solution was cooled, filtered using Whattman filter paper, and stored at 4 °C for further use.

3.2.3 Preparation of *H. undatus* peel extract

Two dragon fruit peels were collected, cleaned and dried in an oven at 55 °C for 2 days. The dried peels were then powdered and stored them in tightly sealed container. A 5 g sample of the peel powder was combined with 100 ml of distilled water in a beaker. The beaker was kept on hot plate to boil for about 4 hours maintaining the temperature range of 80-90 °C using a thermometer. The brownish-yellow colored solution was allowed to cool, filtered using Whattman filter paper, and stored at 4 °C for further analysis.

3.2.4 Synthesis of Iron Oxide NPs using leaf extract

Initially, a solution was prepared in 30 ml distilled water at room temperature by adding $FeCl_2$: $FeCl_3$ precursors by (w/w) ratio as 1:2 and stirred for 30 minutes at 500 rpm. Then, 30 ml of a prepared leaf extract was added that lead to change in color from light brown to brown-black along with continuous stirring of solution. Further, NaOH (2M) was added dropwise as stabilizing agent to adjust the pH around 7-8 making solution dark brown in color and stirred for 2 hours. The dark brown precipitate was collected through filtration,

then washed multiple times with distilled water, and one last with ethanol. Further, it was dried at 55 °C in an oven overnight and brown powder was calcined at 350 °C for 4 hours.

3.2.5 Synthesis of Iron Oxide NPs using peel extract

Initially, a solution of $FeCl_2$ and $FeCl_3$ precursors were made by dissolving (w/w) ratio as 1:2 in 15 ml distilled water, followed by stirring at room temperature for 30 minutes at 500 rpm. There was an addition of 5 ml prepared peel extract converting the color of solution from light brown to brown-black with continuous stirring. Further, NaOH (2M) was added dropwise as stabilizing agent to adjust the pH around 11-12 making solution dark brown in color and stirred for 2 hours. The dark brown precipitate was collected by filtration, washed several times with distilled water and once with ethanol. Finally, it was kept in oven at 55 °C overnight resulting brown powder that was calcined at 350 °C for 3 hours.

3.3 Conclusion

Iron oxide nanoparticles were produced using lemongrass leaf and dragon fruit peel extracts in an environmentally manner applying green approach. The procedure included boiling the plant materials in distilled water to create extracts, combining them with iron precursors, adjusting the pH and resulting into precipitate. This eco-friendly synthesis process provides a sustainable approach for generating iron oxide nanoparticles that could be utilized across different industries.

Chapter 4 Results and Discussions

4.1 X-Ray Diffraction (XRD)

Lemon grass (L): The X-ray diffraction (XRD) pattern of phytonanofabricated iron oxide using lemon grass extract is displayed in Figure 11. The peaks at different 2θ values are observed at 27.54°, 31.88°, 33.31°, 35.79°, 45.60°, 56.57°, 66.35°, 75.36°, 54.10°, and 64.13° and the main peak at 33.31° is observed clearly. The miller indices were assigned as hkl values marked in figure as (012), (104), (110), (113), (024), (116), (122), (214), (300) and (217). The average crystallite size of these nanoparticles was calculated to be 28.35 nm, based on the application of the Scherrer equation. However, XRD is performed to identify the phase composition of material. Although, in this case of nanoparticles were not formed of pure phase of α-Fe_2O_3 as the intensity of another major peak at (110) plane is diminished and new peak appear at (400) plane that corresponds to maghemite (γ-Fe_2O_3) appeared. The reason was the incomplete transformation of phase under the exposure of heat at certain temperature of synthesis followed. It is commonly observed phenomenon as phase transformation is the function of temperature **(Pavani Katikaneani 2016)**.

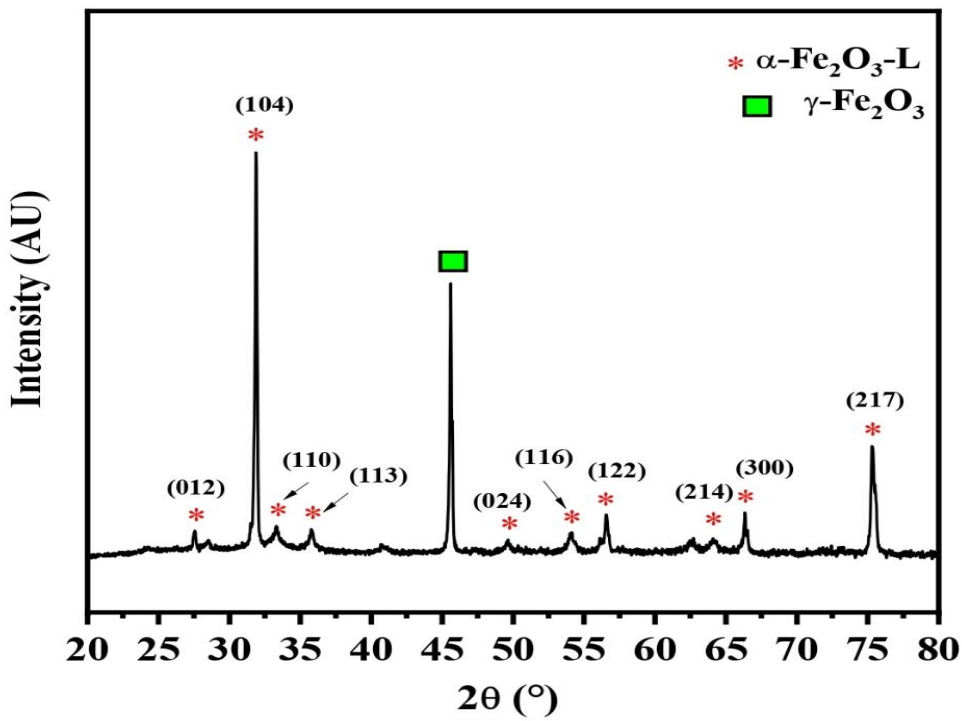

Figure 11: X-ray diffraction pattern showing miller indices of iron oxide nanoparticles synthesized using lemon grass leaf extract.

Dragon Fruit (D): The X-ray diffraction analysis of iron oxide nanoparticles involving dragon fruit peel extract as reducing agent is presented in Figure 12. The pattern exhibits the peaks at 2θ values of 33.01°, 35.48°, 49.41°, 53.99°, 62.66°, and 63.83°, which can be further assigned to the corresponding crystallographic planes such as (012), (104), (110), (113), (024), (116), (122), (214), (300) and (217). This observation has been verified using JCPDS database **(Rui Han 2014)**. The average crystallite size of these nanoparticles was calculated to be 9.55 nm using Scherrer equation. Somehow, these nanoparticles were prepared peel extract of dragon fruit that resulted in nearly pure phase of α-Fe_2O_3 but as observed from the pattern, there was a decrease of major peak intensity at (104) plane than (110) plane. It indicates that broad peaks are observed for the structures prepared at higher pH and the orientation of crystalline structure did not align to the direction of crystal growth **(Chulwoo Park 2016)**.

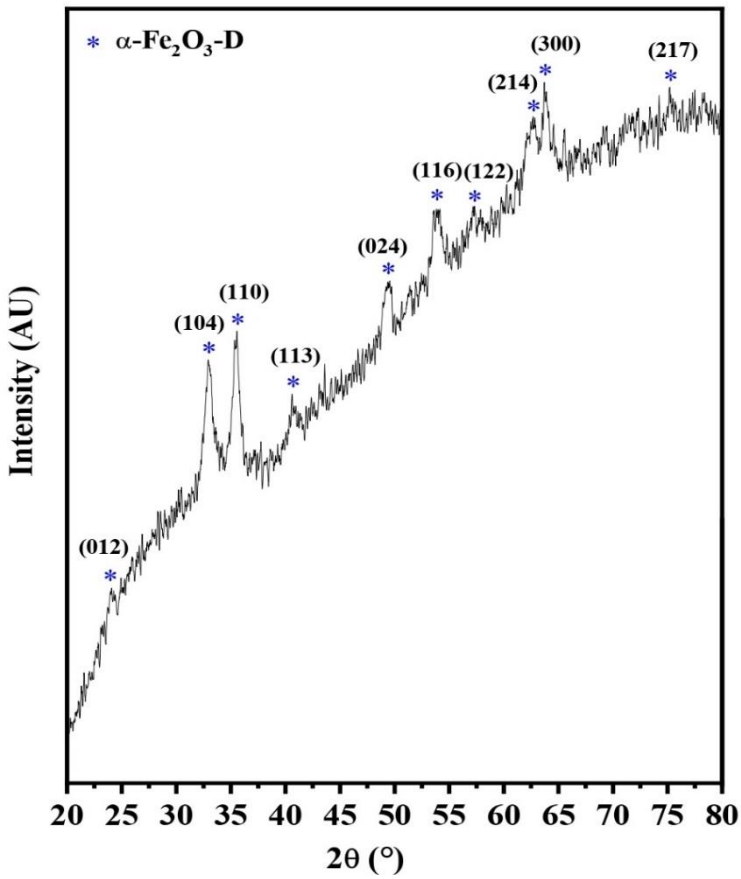

Figure 12: X-ray diffraction pattern showing miller indices of iron oxide nanoparticles created using dragon fruit peel extract.

4.2 Scanning Electron Microscopy (SEM) with Energy Dispersive X-Ray Analysis (EDX)

Lemon grass (L): SEM technique was employed to examine the size and morphology of synthesized nanoparticles. Figure 13 (a) represents the lemon grass leaf extract prepared iron oxide NPs. The figure revealed that nanoparticles were nearly cubical shaped particles. The accumulation on the particle surface may be ascribed to the biological compounds in proximity.

EDX elemental inspection was performed to ascertain the presence of constituent elements in the produced materials, thereby confirming the existence of Fe, O in the given sample of nanoparticles. The EDS spectrum in figure 14 demonstrated the homogenous placement of Fe, O, C and N elements in synthesized material. The samples contain. In Table 2, elements along with weight % and certain atomic % is shown for iron oxide NPs.

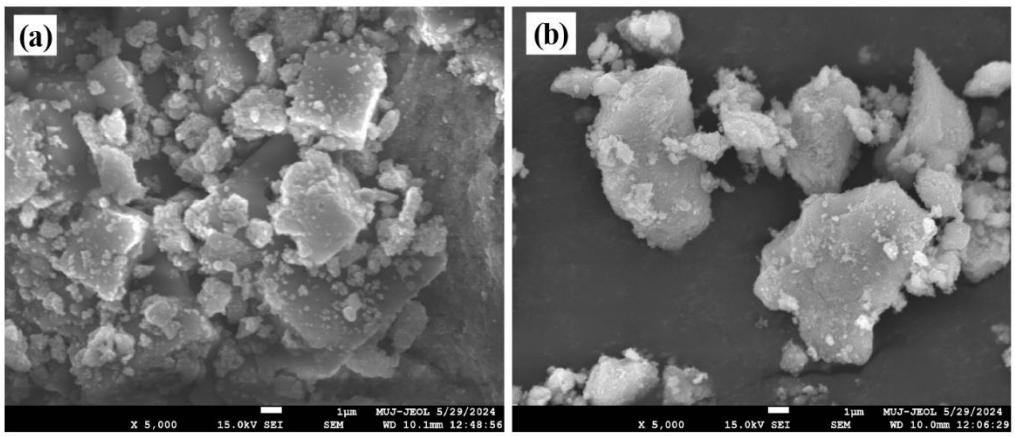

Figure 13: SEM image of iron oxide nanoparticles synthesized using (a) lemon grass leaf extract and (b) dragon fruit peel extract.

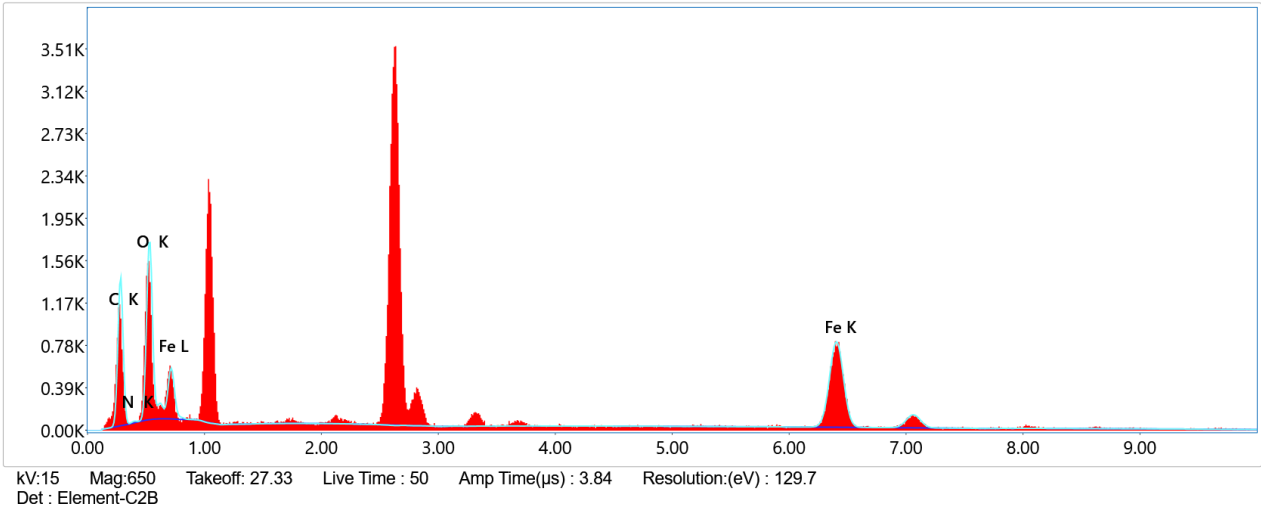

Figure 14: EDX analysis of iron oxide nanoparticles prepared using lemon grass leaf extract.

Table 2: Elemental distribution by weight % and atomic% of iron oxide prepared sample using lemon grass leaf extract.

Element (L)	Weight (%)	Atomic (%)
Fe	30.1	9.2
O	24.8	26.5
C	44.5	63.5
N	0.6	0.7

Dragon Fruit (D): As illustrated in Figure 13 (b), representing morphology of iron oxide NPs prepared using dragon fruit peel extract. The image displayed irregular, agglomerated structure of nanoparticles. This aggregation may be due the biological components of extract on the surface.

Through EDX examination, it is proved that Fe, O elements were present in the given sample of nanoparticles. Figure 15 represented the energy dispersion x-ray spectroscopy (EDS) spectrum of the nanoparticles containing elements such as Fe, O, C and N. In Table 3, elements along with weight % and certain atomic % is shown for iron oxide NPs.

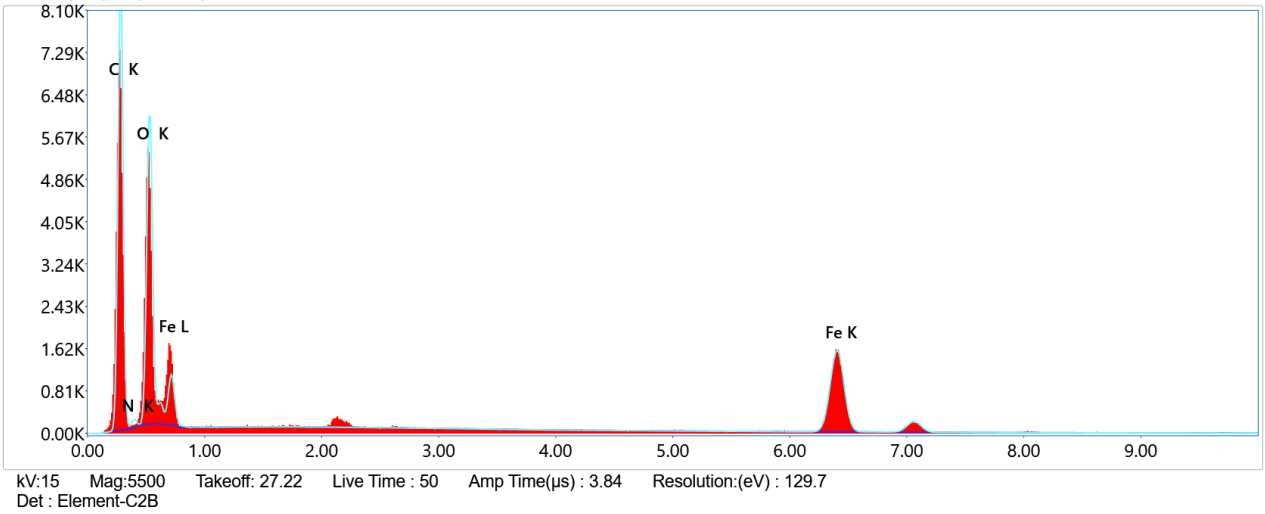

Figure 15: EDX analysis of iron oxide nanoparticles prepared using dragon fruit peel extract.

Table 3: Elemental distribution by weight % and atomic% of iron oxide prepared sample using dragon fruit peel extract.

Element	Weight (%)	Atomic (%)
Fe	14.9	3.9
O	27.3	25.2
C	56.0	68.9
N	1.8	1.9

4.3 Fourier-Transform Infrared Spectroscopy (FTIR)

The FTIR spectrum in figure 16 depicts the characteristics of biosynthesized iron oxide NPs prepared using two plant sources extracts where L represent the lemon grass leaf extract and D is the dragon fruit peel extract respectively. In case of spectrum of sample L, represents a broad peak at 3391 cm^{-1}, attributed to the -OH vibration. The peaks at 2948 cm^{-1} and 2872 cm^{-1} relative to symmetric stretching of C-H. The band from 1700-1400 cm^{-1} refers to C=O stretching where 1733 cm^{-1} and 1411 cm^{-1} are symmetric and 1627 cm^{-1} is asymmetric vibration respectively. There is another band in the range of 1200-1000 cm^{-1} associated with C-O-C stretching with prominent peaks at 1281 and 1070 cm^{-1} for asymmetric and symmetric vibration along with 1127 cm^{-1} representing C-O stretching. There is small signal at 723 cm^{-1} that might show out of plane C-H or O-H bending. The spectrum reveals

characteristic peaks at 531 and 454 cm^{-1} that confirms the Fe-O bond **(M. Alagiri 2014) (Mohamed Bilal Goudjil 2024).**

The infrared spectrum of sample D represented in figure 16 displayed a small signal at 3391 cm^{-1} which was identified as -OH functional group. The peaks at 2948 and 2872 cm^{-1} can be attributed to C-H symmetric stretching. The region between 1700-1400 cm^{-1} refers to C=O stretching where 1733 and 1627 cm^{-1} is symmetric and asymmetric vibration respectively. Additionally, the band from 1200-1000 cm^{-1} was allocated to C-O-C stretching, with prominent peaks at 1272 and 1070 cm^{-1} for asymmetric and symmetric vibrations, along with a peak at 1127 cm^{-1} representing C-O stretching. The signal at 723 cm^{-1} might indicate out-of-plane C-H or O-H bending of bonds. The spectrum reveals characteristic peaks at 531 and 435 cm^{-1} that confirms the presence of iron-oxygen (Fe-O) bond **(M. Alagiri 2014) (Mohamed Bilal Goudjil 2024)**.

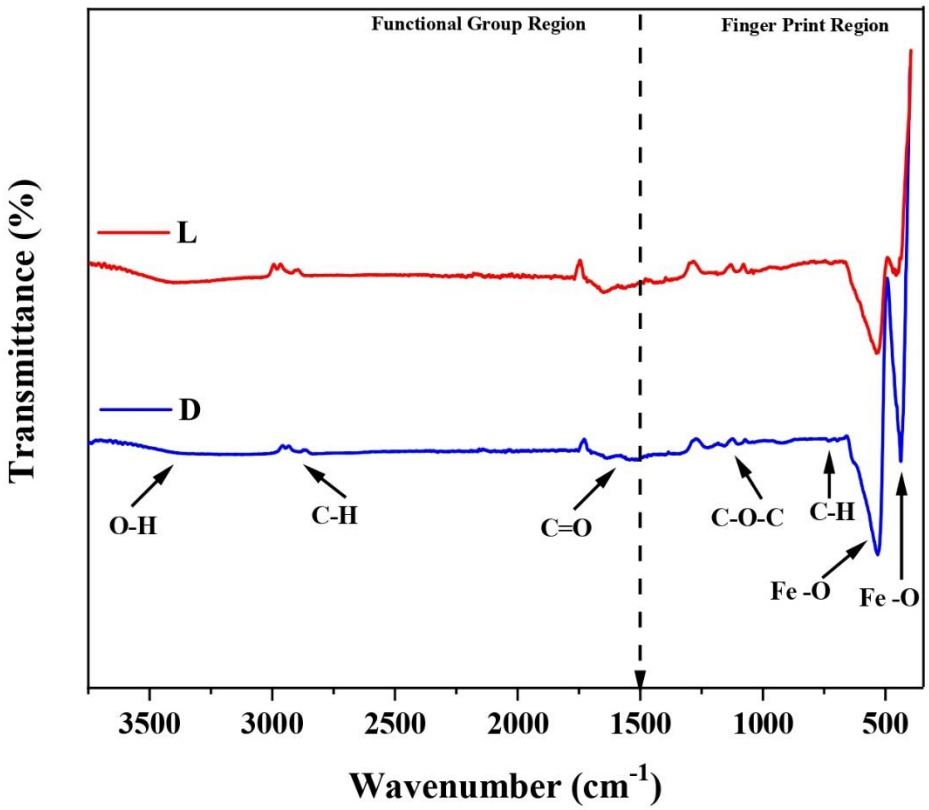

Figure 16: FTIR spectrum of iron oxide nanoparticles prepared using lemon grass leaf (red line) and dragon fruit peel (blue line) extract respectively.

4.4 Zeta Potential

Zeta potential determines the colloidal stability of nanoparticles in suspension, and indicates their surface charge. Figure 12 and 13 shows the plot of Zeta potential of iron oxide nanoparticles prepared using lemon grass leaf and dragon fruit peel extract respectively. According to literature, higher the value of Zeta potential indicates greater colloidal stability for the nanoparticles dispersed in the solution. The values reported in case of lemon grass prepared iron oxide nanoparticles is -5.64 mV and for dragon fruit peel extract it is -2.39 mV, which is lower than former value.

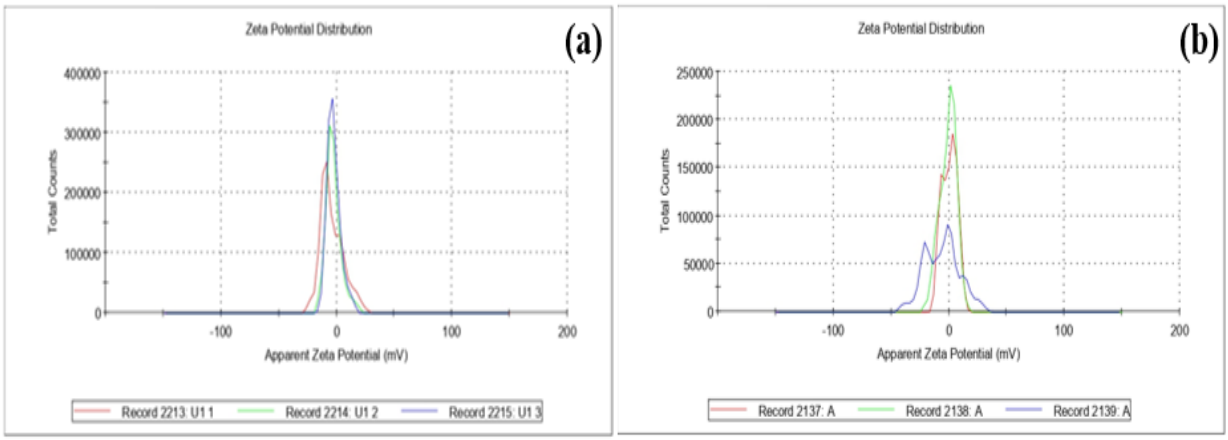

Figure 17: Zeta potential plot of iron oxide nanoparticles synthesized using (a) lemon grass leaf extract and (b) dragon fruit peel extract.

4.5 Vibrating-sample magnetometry (VSM)

The room temperature magnetization-field (MH) curves have been plotted for the biosynthesized iron oxide nanoparticles using two plant sources, as represented by figures 14 and 15. The measurements were performed in the range of -10 kOe to 10 kOe, with 14 mg of each sample, to investigate diversified magnetic performance of the samples. The

responding magnetization values (M_s, M_r and H_c) has also been shown in the figure. The iron oxide nanoparticles synthesized using leaf extract of lemon grass revealed M_s as 0.65 emu/g and coercivity of 39.28 Oe. Similarly, in the case of dragon fruit peel extract synthesized nanoparticles showed a comparable magnetic saturation of 0.67 emu/g and a H_c of 35.73 Oe.

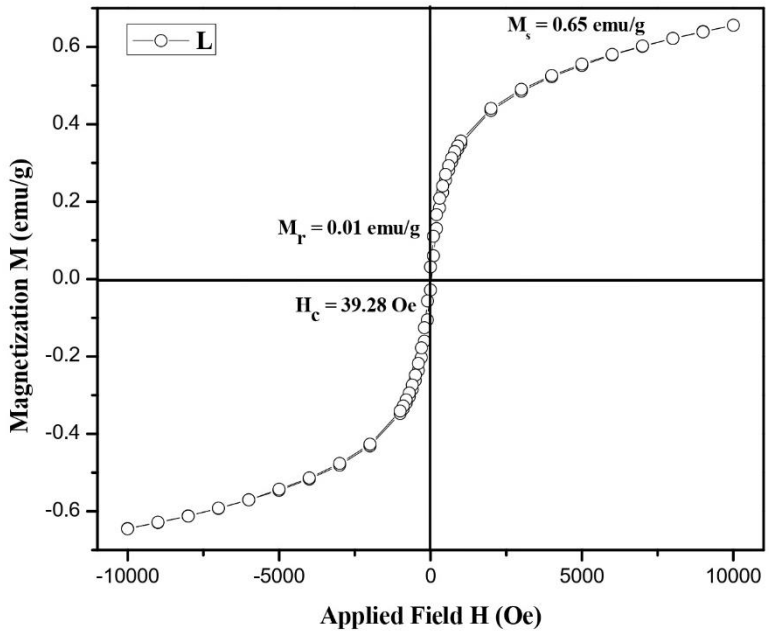

Figure 18: Room temperature MH curve for the of iron oxide nanoparticles prepared using lemon grass leaf extract.

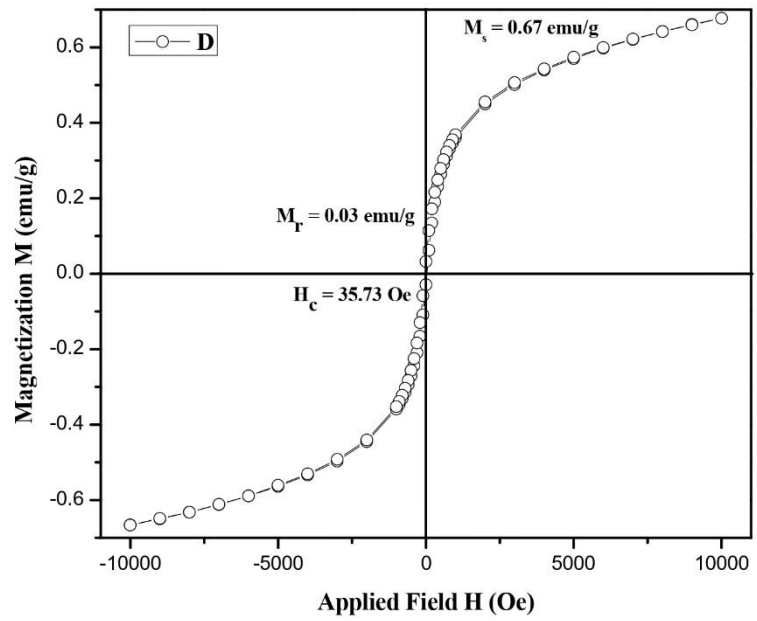

Figure 19: Room temperature MH curve for the of iron oxide nanoparticles prepared using dragon fruit peel extract.

4.6 Conclusion

This section presents the findings from the characterization techniques performed on the two samples of iron oxide nanoparticles. Structural analysis was done by XRD that confirmed the synthesis of iron oxide nanoparticles having crystallite size 28.35 and 9.55 nm in case of particles prepared using leaf and peel extract respectively. Morphology of the nanoparticles were confirmed from SEM as nearly cubical shaped and irregular shaped in case of particles prepared using leaf and peel extract respectively. EDX elemental analysis confirmed the presence of elements Fe and O along with C and N presence and FTIR study confirmed the presence of Fe-O band in both the samples of nanoparticles. Zeta potential was reported as -5.64 and -2.39 mV in case of nanoparticles prepared using leaf and peel extract respectively. MH curves showed the weakly ferromagnetic behaviour in both the samples of nanoparticles.

Chapter 5 Photocatalytic activity of Iron Oxide NPs synthesized using *C. citratus* leaf extract

5.1 Methylene Blue (MB) Dye Degradation

Dyes are categorized into anionic, cationic and non-ionic types based on their distinct chromophore and auxochrome groups. They can also be classified by color, chemical structure or features like basic, acidic, direct, naphtha, mordant azo, vat reactive dissolve, and sulphur dyes with azo dyes being most commonly used at present. Derived from plants or synthetic sources, certain natural characteristics distinguish them **(Muhammad Farooque Lanjwani 2024)**. Cationic dyes like methylene blue, rhodamine 6G (Rh6G) and malachite green contain functional groups that become positively charged ions in aqueous solutions while anionic dyes such as eosin Y, congo red and methyl orange interact efficiently with photocatalysts through hydrophilic surfaces due to sulfonic acid, anionic or carbozolic acids functionalities respectively. Methylene blue known for its toxic nature is extensively applied in dyeing leather wood cotton production processes despite posing health hazards including increased heart rate nausea discomfort **(Peter Olusakin Oladoye 2022)**.

Various methods have been developed to eliminate dyes from industrial effluents and water bodies in order to reduce their harmful effects on living organisms. The effectiveness of these techniques relies on the characteristics of the dyes, impurities, and composition of the wastewater. Anionic dyes are highly soluble in water and difficult to remove using traditional approaches, while biological treatments may not effectively address acidic and reactive dyes. Non-ionic or disperse dyes have condensed aromatic ring systems that do not dissociate in water solutions and exhibit aversion to decomposition. However, certain cationic dyes such as methylene blue can be successfully removed through processes like adsorption and advanced oxidation **(Akil Ahmad 2015)**.

As previously discussed in Chapter 1: Introduction and Literature Survey, photocatalytic dye degradation, using transition metal oxide nanoparticles, is a prime option for methylene blue dye removal in wastewater remediation.

5.2 Procedure

A pre-assembled chamber served as the photoreactor for the photocatalytic experiment. A UV-emitting 125 W mercury vapor lamp radiation-based investigation, a 105 mL solution of MB with an initial concentration of 20 ppm using water as solvent. The iron oxide nanoparticles sample prepared using lemon grass leaf extract weighing 50 mg were introduced as a photocatalyst into the dye solution with continuous stirring. An initial half-hour period took place without turning on the lamp in dark conditions to allow adsorption/desorption equilibrium before exposure to light (pre-irradiation). Following this, upon switching on the UV lamp, all subsequent procedures were carried out under its illumination. Every thirty minutes thereafter, about 3 mL each were taken from suspension and centrifuged to separate the catalyst, after which their absorbance levels were measured.

The MB degradation efficiency was evaluated using a UV-Vis spectrophotometer. The absorption spectrum exhibited peaks in the 600-700 nm range, indicating the presence of a π-conjugated system, suggesting MB degradation. Furthermore, based on the Beer-Lambert law, the absorbance of the solution is directly linked to the concentration of MB. This relationship allows for the determination of MB oxidation efficiency using the equation:

$$R = \frac{L_o - L_t}{L_o} \times 100\%$$

where the initial concentration of MB solution is represented by L_o represents and the concentration of MB during the irradiation process is denoted by L_t **(Zatil Amali Che Ramli 2014).**

5.3 Observations

The study was focused on examining the breakdown of MB dye using iron oxide nanoparticles produced with lemon grass leaf extract. The research assessed their ability to adsorb and facilitate the breakdown of MB under ultraviolet radiation. The main absorption peak i.e maximum wavelength (λ_{max}) of methylene blue dye is 664 nm **(Mohamed Bilal Goudjil 2024).** The photodegradation was inspected at different time gaps of dye under UV

lamp irradiation, with concentration of the catalyst maintained at 50mg/L. The findings revealed that before the lamp was switched on during the duration of 30 mins, there was less than 1% adsorption of dye by catalyst. After 30 mins UV lamp was turned on leading to increase in degradation of dye. The figure 20 represent that the majority of the MB colorant i.e. more than 90% was eliminated within 120 minutes and more than 99% was degraded within 150 minutes.

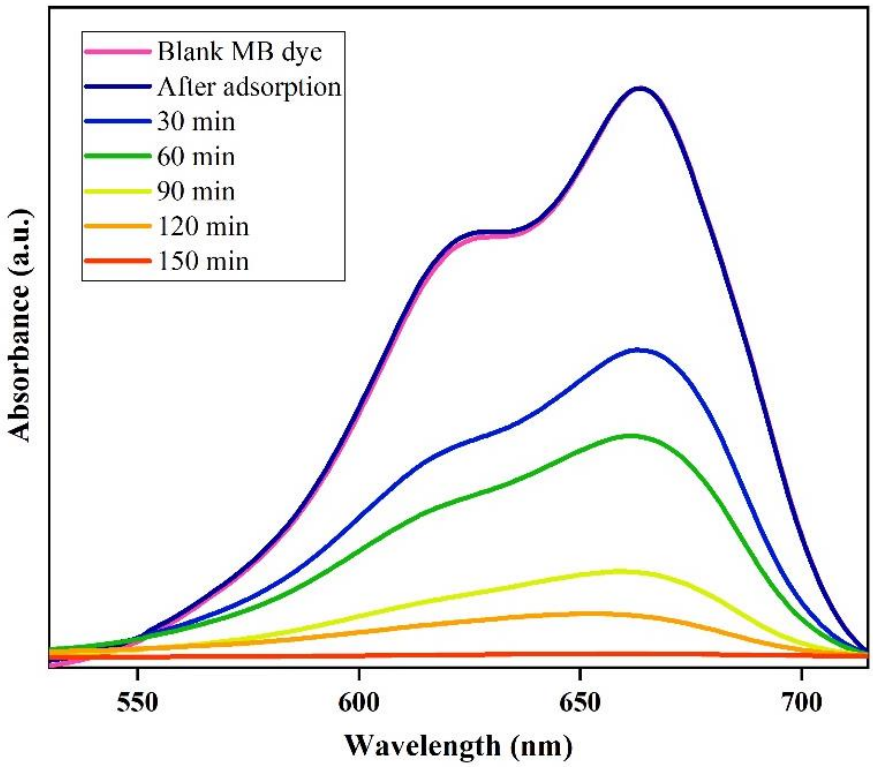

Figure 20: UV-visible spectroscopy analysis of green synthesized iron oxide nanoparticles prepared using lemon grass leaf extract representing photocatalytic MB dye decomposition activity.

5.4 Proposed Mechanism

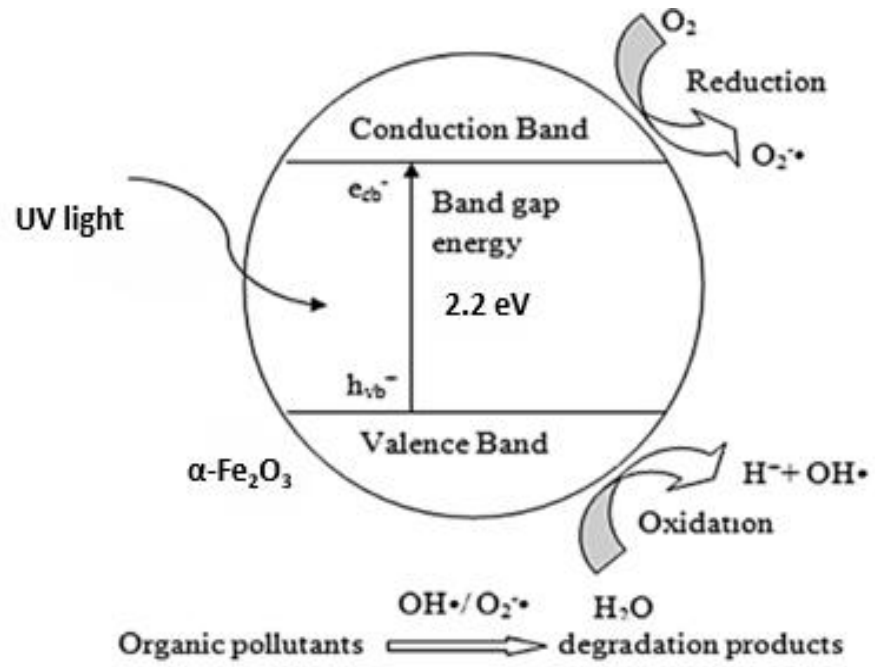

Figure 21: Proposed mechanism of photocatalysis by iron oxide nanoparticles prepared using lemon grass (*Cymbopogon citratus*) leaf extract.

5.5 Conclusion

Photocatalysis has emerged as promising technology for environmental remediation, especially in the degradation of organic pollutants in wastewater. The capacity to operate UV light and transform into chemical energy through a sustainable approach renders it an attractive option for addressing pollution. This chapter summarized the photocatalytic efficiency was examined of lemon grass leaf extract prepared iron oxide nanoparticles that degraded 93% MB dye under UV lamp irradiation within 120 minutes.

Chapter 6 Conclusion of Dissertation

6.1 Conclusion

Iron oxide nanoparticles were synthesised under green approach by using two plant sources such that lemongrass (*C. citratus*) leaf extract and dragon fruit (*H. undatus*) peel extract as reducing and capping agents. Structural analysis was confirmed through XRD analysis having crystallite size 28.35 and 9.55 nm in case of iron oxide nanoparticles prepared using leaf and peel extract respectively. Morphology of the nanoparticles were confirmed from SEM as nearly cubical shaped and irregular shaped in case of particles prepared using leaf and peel extract respectively. EDX elemental analysis confirmed the presence of particles Fe and O along with C and N presence and FTIR study verified the existence of iron-oxygen (Fe-O) vibrations in both the samples of nanoparticles. Zeta potential was reported as -5.64 and -2.39 mV in case of nanoparticles prepared using leaf and peel extract respectively. MH curves showed the weakly ferromagnetic behaviour in both the samples of nanoparticles. Photocatalytic efficiency was examined of lemon grass leaf extract prepared iron oxide nanoparticles that degraded 93% MB dye under UV lamp irradiation within 120 minutes.

6.2 Scope for Future Work

The green-synthesized metal oxide nanoparticles using plant extracts, bacteria, fungi, and algae has shown promising future for the degradation of colorant dye, as it offers a sustainable and eco-friendly solution to water pollution. This method reduces use of harmful chemicals & minimizes the negative impact on environment. The experimental analysis was performed under UV lamp for photocatalytic test activity which shows effect only under UV region, so visible light should be promising candidate as energy source. With biosynthesized iron oxide nanoparticles, water splitting application to produce fuel can also be investigated further due to magnetic properties, eco-friendly samples, recoverable and reusability.

References:

[1] Y. Getahun, J. Gardea-Torresdey, F. S. Manciu, X. Li, and A. A. El-Gendy, "Green Synthesized Superparamagnetic Iron Oxide Nanoparticles for Water Treatment with Alternative Recyclability," 2022.

[2] A. A. Yaqoob, T. Parveen, K. Umar, and M. N. M. Ibrahim, "Role of nanomaterials in the treatment of wastewater: A review," *Water (Switzerland)*, vol. 12, no. 2. MDPI AG, Feb. 01, 2020. doi: 10.3390/w12020495.

[3] B. Pandey, P. Singh, and V. Kumar, "Photocatalytic-sorption processes for the removal of pollutants from wastewater using polymer metal oxide nanocomposites and associated environmental risks," *Environmental Nanotechnology, Monitoring and Management*, vol. 16. Elsevier B.V., Dec. 01, 2021. doi: 10.1016/j.enmm.2021.100596.

[4] J. Iyyappan, B. Gaddala, R. Gnanasekaran, M. Gopinath, D. Yuvaraj, and V. Kumar, "Critical review on wastewater treatment using photo catalytic advanced oxidation process: Role of photocatalytic materials, reactor design and kinetics," *Case Studies in Chemical and Environmental Engineering*, vol. 9, Jun. 2024, doi: 10.1016/j.cscee.2023.100599.

[5] M. Noman *et al.*, "Use of biogenic copper nanoparticles synthesized from a native Escherichia sp. as photocatalysts for azo dye degradation and treatment of textile effluents," *Environmental Pollution*, vol. 257, Feb. 2020, doi: 10.1016/j.envpol.2019.113514.

[6] C. Alex Mbachu, A. Kamoru Babayemi, T. Chinedu Egbosiuba, J. Ifeanyichukwu Ike, I. Jacinta Ani, and S. Mustapha, "Green synthesis of iron oxide nanoparticles by Taguchi design of experiment method for effective adsorption of methylene blue and methyl orange from textile wastewater," *Results in Engineering*, vol. 19, Sep. 2023, doi: 10.1016/j.rineng.2023.101198.

[7] M. F. Lanjwani, M. Tuzen, M. Y. Khuhawar, and T. A. Saleh, "Trends in photocatalytic degradation of organic dye pollutants using nanoparticles: A review," *Inorganic Chemistry Communications*, vol. 159. Elsevier B.V., Jan. 01, 2024. doi: 10.1016/j.inoche.2023.111613.

[8] S. Dutta *et al.*, "Contamination of textile dyes in aquatic environment: Adverse impacts on aquatic ecosystem and human health, and its management using bioremediation," *Journal of Environmental Management*, vol. 353. Academic Press, Feb. 27, 2024. doi: 10.1016/j.jenvman.2024.120103.

[9] H. A. Maddah, "Predicting Optimum Dilution Factors for BOD Sampling and Desired Dissolved Oxygen for Controlling Organic Contamination in Various Wastewaters," *International Journal of Chemical Engineering*, vol. 2022, 2022, doi: 10.1155/2022/8637064.

[10] M. Behera, J. Nayak, S. Banerjee, S. Chakrabortty, and S. K. Tripathy, "A review on the treatment of textile industry waste effluents towards the development of efficient mitigation strategy: An integrated system design approach," *J Environ Chem Eng*, vol. 9, no. 4, Aug. 2021, doi: 10.1016/j.jece.2021.105277.

[11] B. Sarkodie, J. Amesimeku, C. Frimpong, E. K. Howard, Q. Feng, and Z. Xu, "Photocatalytic degradation of dyes by novel electrospun nanofibers: A review," *Chemosphere*, vol. 313. Elsevier Ltd, Feb. 01, 2023. doi: 10.1016/j.chemosphere.2022.137654.

[12] V. K. Saharan, D. V. Pinjari, P. R. Gogate, and A. B. Pandit, "Advanced Oxidation Technologies for Wastewater Treatment: An Overview," in *Industrial Wastewater Treatment, Recycling and Reuse*, Elsevier Inc., 2014, pp. 141–191. doi: 10.1016/B978-0-08-099968-5.00003-9.

[13] C. R. Holkar, A. J. Jadhav, D. V. Pinjari, N. M. Mahamuni, and A. B. Pandit, "A critical review on textile wastewater treatments: Possible approaches," *Journal of Environmental Management*, vol. 182. Academic Press, pp. 351–366, Nov. 01, 2016. doi: 10.1016/j.jenvman.2016.07.090.

[14] Y. Deng and R. Zhao, "Advanced Oxidation Processes (AOPs) in Wastewater Treatment," *Current Pollution Reports*, vol. 1, no. 3. Springer, pp. 167–176, Sep. 01, 2015. doi: 10.1007/s40726-015-0015-z.

[15] P. K. Pandis *et al.*, "Key Points of Advanced Oxidation Processes (AOPs) for Wastewater, Organic Pollutants and Pharmaceutical Waste Treatment: A Mini Review," *ChemEngineering*, vol. 6, no. 1. MDPI, Feb. 01, 2022. doi: 10.3390/chemengineering6010008.

[16] M. A. Al-Nuaim, A. A. Alwasiti, and Z. Y. Shnain, "The photocatalytic process in the treatment of polluted water," *Chemical Papers*, vol. 77, no. 2. Springer Science and Business Media Deutschland GmbH, pp. 677–701, Feb. 01, 2023. doi: 10.1007/s11696-022-02468-7.

[17] D. D. Thongam and H. Chaturvedi, "Advances in nanomaterials for heterogeneous photocatalysis," *Nano Express*, vol. 2, no. 1. Institute of Physics, Mar. 01, 2021. doi: 10.1088/2632-959X/abeb8d.

[18] N. Ahmad *et al.*, "Visible light-conducting polymer nanocomposites as efficient photocatalysts for the treatment of organic pollutants in wastewater," *Journal of*

Environmental Management, vol. 295. Academic Press, Oct. 01, 2021. doi: 10.1016/j.jenvman.2021.113362.

[19] Khan, Mohammad Mansoob. *Theoretical Concepts of Photocatalysis*. Elsevier, 2023.

[20] A. Q. Malik *et al.*, "An Overview on Magnetic Separable Spinel as a Promising Materials for Photocatalysis and Waste Water Treatment," *ES Energy and Environment*, vol. 19, Mar. 2023, doi: 10.30919/esee8c744.

[21] M. B. Tahir, T. Iqbal, M. Rafique, M. S. Rafique, T. Nawaz, and M. Sagir, "Nanomaterials for photocatalysis," in *Nanotechnology and Photocatalysis for Environmental Applications*, Elsevier, 2020, pp. 65–76. doi: 10.1016/b978-0-12-821192-2.00005-x.

[22] R. Tomar, A. A. Abdala, R. G. Chaudhary, and N. B. Singh, "Photocatalytic degradation of dyes by nanomaterials," in *Materials Today: Proceedings*, Elsevier Ltd, 2020, pp. 967–973. doi: 10.1016/j.matpr.2020.04.144.

[23] A. Thirunavukkarasu, R. Nithya, and R. Sivashankar, "A review on the role of nanomaterials in the removal of organic pollutants from wastewater," *Reviews in Environmental Science and Biotechnology*, vol. 19, no. 4. Springer Science and Business Media B.V., pp. 751–778, Dec. 01, 2020. doi: 10.1007/s11157-020-09548-8.

[24] S. Zahmatkesh, M. Hajiaghaei-Keshteli, A. Bokhari, S. Sundaramurthy, B. Panneerselvam, and Y. Rezakhani, "Wastewater treatment with nanomaterials for the future: A state-of-the-art review," *Environ Res*, vol. 216, Jan. 2023, doi: 10.1016/j.envres.2022.114652.

[25] H. Sadegh *et al.*, "The role of nanomaterials as effective adsorbents and their applications in wastewater treatment," *Journal of Nanostructure in Chemistry*, vol. 7, no. 1. Springer Medizin, pp. 1–14, Mar. 01, 2017. doi: 10.1007/s40097-017-0219-4.

[26] B. Barik, P. S. Nayak, and P. Dash, "Nanomaterials in wastewater treatments," in *Nanotechnology in the Beverage Industry: Fundamentals and Applications*, Elsevier, 2020, pp. 185–206. doi: 10.1016/B978-0-12-819941-1.00007-9.

[27] H. Saleem and S. J. Zaidi, "Developments in the application of nanomaterials for water treatment and their impact on the environment," *Nanomaterials*, vol. 10, no. 9. MDPI AG, pp. 1–39, Sep. 01, 2020. doi: 10.3390/nano10091764.

[28] W. Umar *et al.*, "Use of nanotechnology for wastewater treatment: Potential applications, advantages, and limitations," in *Sustainable Nanotechnology for Environmental Remediation*, Elsevier, 2022, pp. 223–272. doi: 10.1016/B978-0-12-824547-7.00002-3.

[29] P. Xu *et al.*, "Use of iron oxide nanomaterials in wastewater treatment: A review," *Science of The Total Environment*, vol. 424, pp. 1–10, May 2012, doi: 10.1016/j.scitotenv.2012.02.023.

[30] L. Madhura, S. Singh, S. Kanchi, M. Sabela, K. Bisetty, and Inamuddin, "Nanotechnology-based water quality management for wastewater treatment," *Environmental Chemistry Letters*, vol. 17, no. 1. Springer Verlag, pp. 65–121, Mar. 01, 2019. doi: 10.1007/s10311-018-0778-8.

[31] T. A. Aragaw, F. M. Bogale, and B. A. Aragaw, "Iron-based nanoparticles in wastewater treatment: A review on synthesis methods, applications, and removal mechanisms," *Journal of Saudi Chemical Society*, vol. 25, no. 8. Elsevier B.V., Aug. 01, 2021. doi: 10.1016/j.jscs.2021.101280.

[32] J. Gómez-Pastora, S. Dominguez, E. Bringas, M. J. Rivero, I. Ortiz, and D. D. Dionysiou, "Review and perspectives on the use of magnetic nanophotocatalysts (MNPCs) in water treatment," *Chemical Engineering Journal*, vol. 310, pp. 407–427, Feb. 2017, doi: 10.1016/j.cej.2016.04.140.

[33] S. Shukla, R. Khan, and A. Daverey, "Synthesis and characterization of magnetic nanoparticles, and their applications in wastewater treatment: A review," *Environmental Technology and Innovation*, vol. 24. Elsevier B.V., Nov. 01, 2021. doi: 10.1016/j.eti.2021.101924.

[34] R. Bhateria and R. Singh, "A review on nanotechnological application of magnetic iron oxides for heavy metal removal," *Journal of Water Process Engineering*, vol. 31. Elsevier Ltd, Oct. 01, 2019. doi: 10.1016/j.jwpe.2019.100845.

[35] B. E. Keshta *et al.*, "State of the art on the magnetic iron oxide Nanoparticles: Synthesis, Functionalization, and applications in wastewater treatment," *Results Chem*, vol. 7, Jan. 2024, doi: 10.1016/j.rechem.2024.101388.

[36] J. Tuček *et al.*, "Zeta-Fe 2 O 3 - A new stable polymorph in iron(III) oxide family," *Sci Rep*, vol. 5, Oct. 2015, doi: 10.1038/srep15091.

[37] A. Ali *et al.*, "Synthesis, characterization, applications, and challenges of iron oxide nanoparticles," *Nanotechnology, Science and Applications*, vol. 9. Dove Medical Press Ltd, pp. 49–67, Aug. 19, 2016. doi: 10.2147/NSA.S99986.

[38] A. S. Teja and P. Y. Koh, "Synthesis, properties, and applications of magnetic iron oxide nanoparticles," *Progress in Crystal Growth and Characterization of Materials*, vol. 55, no. 1–2. pp. 22–45, Mar. 2009. doi: 10.1016/j.pcrysgrow.2008.08.003.

[39] C. N. Lininger *et al.*, "Energetics of Lithium Insertion into Magnetite, Defective Magnetite, and Maghemite," *Chemistry of Materials*, vol. 30, no. 21, pp. 7922–7937, Nov. 2018, doi: 10.1021/acs.chemmater.8b03544.

[40] F. Kraushofer *et al.*, "Atomic-Scale Structure of the Hematite α-Fe2O3(11-02) 'r-Cut' Surface," *Journal of Physical Chemistry C*, vol. 122, no. 3, pp. 1657–1669, Jan. 2018, doi: 10.1021/acs.jpcc.7b10515.

[41] H. Mirzaei and M. Darroudi, "Zinc oxide nanoparticles: Biological synthesis and biomedical applications," *Ceram Int*, vol. 43, no. 1, pp. 907–914, 2017, doi: 10.1016/j.ceramint.2016.10.051.

[42] A. P. Lagrow *et al.*, "Unravelling the growth mechanism of the co-precipitation of iron oxide nanoparticles with the aid of synchrotron X-Ray diffraction in solution," *Nanoscale*, vol. 11, no. 14, pp. 6620–6628, Apr. 2019, doi: 10.1039/c9nr00531e.

[43] B. Issa, I. M. Obaidat, B. A. Albiss, and Y. Haik, "Magnetic nanoparticles: Surface effects and properties related to biomedicine applications," *International Journal of Molecular Sciences*, vol. 14, no. 11. pp. 21266–21305, Oct. 25, 2013. doi: 10.3390/ijms141121266.

[44] H. Guo and A. S. Barnard, "Naturally occurring iron oxide nanoparticles: Morphology, surface chemistry and environmental stability," *J Mater Chem A Mater*, vol. 1, no. 1, pp. 27–42, Jan. 2013, doi: 10.1039/c2ta00523a.

[45] J. Singh, T. Dutta, K.-H. Kim, M. Rawat, P. Samddar, and P. Kumar, "'Green' synthesis of metals and their oxide nanoparticles: applications for environmental remediation," *J Nanobiotechnology*, vol. 16, no. 1, p. 84, Dec. 2018, doi: 10.1186/s12951-018-0408-4.

[46] N. A. I. Md Ishak, S. K. Kamarudin, and S. N. Timmiati, "Green synthesis of metal and metal oxide nanoparticles via plant extracts: an overview," *Mater Res Express*, vol. 6, no. 11, p. 112004, Oct. 2019, doi: 10.1088/2053-1591/ab4458.

[47] J. Pathak *et al.*, "Exploring the Paradigm of Phyto-Nanofabricated Metal Oxide Nanoparticles: Recent Advancements, Applications, and Challenges," *Molecular Biotechnology*. Springer, 2023. doi: 10.1007/s12033-023-00799-8.

[48] J. Jeevanandam *et al.*, "Green approaches for the synthesis of metal and metal oxide nanoparticles using microbial and plant extracts," *Nanoscale*, vol. 14, no. 7, pp. 2534–2571, 2022, doi: 10.1039/d1nr08144f.

[49] A. Mohamed and E. Shafey, "Green synthesis of metal and metal oxide nanoparticles from plant leaf extracts and their applications: A review," pp. 304–339, 2020.

[50] R. Sharma and A. Tripathi, "Green synthesis of nanoparticles and its key applications in various sectors," *Mater Today Proc*, vol. 48, pp. 1626–1632, 2022, doi: 10.1016/j.matpr.2021.09.512.

[51] M. Castro-Puyana, M. L. Marina, and M. Plaza, "Water as green extraction solvent: Principles and reasons for its use," *Curr Opin Green Sustain Chem*, vol. 5, pp. 31–36, Jun. 2017, doi: 10.1016/j.cogsc.2017.03.009.

[52] Priya, Naveen, K. Kaur, and A. K. Sidhu, "Green Synthesis: An Eco-friendly Route for the Synthesis of Iron Oxide Nanoparticles," *Frontiers in Nanotechnology*, vol. 3, Jun. 2021, doi: 10.3389/fnano.2021.655062.

[53] K. Q. Jabbar, A. A. Barzinjy, and S. M. Hamad, "Iron oxide nanoparticles: Preparation methods, functions, adsorption and coagulation/flocculation in wastewater treatment," *Environmental Nanotechnology, Monitoring and Management*, vol. 17. Elsevier B.V., May 01, 2022. doi: 10.1016/j.enmm.2022.100661.

[54] O. A. Lawal, A. L. Ogundajo, N. O. Avoseh, and I. A. Ogunwande, "Cymbopogon citratus," in *Medicinal Spices and Vegetables from Africa: Therapeutic Potential Against Metabolic, Inflammatory, Infectious and Systemic Diseases*, Elsevier Inc., 2017, pp. 397–423. doi: 10.1016/B978-0-12-809286-6.00018-2.

[55] M. T. Mohammed and M. A. Mahdi, "Biosynthesis of Gold nanoparticles using Dragon fruit and study their biochemical properties," 2019. doi: http://dx.doi.org/10.13140/RG.2.2.23383.75681.

[56] S. Shyamalagowri, P. Charles, J. Manjunathan, M. Kamaraj, R. Anitha, and A. Pugazhendhi, "In vitro anticancer activity of silver nanoparticles phyto-fabricated by Hylocereus undatus peel extracts on human liver carcinoma (HepG2) cell lines," *Process Biochemistry*, vol. 116, pp. 17–25, May 2022, doi: 10.1016/j.procbio.2022.02.022.

[57] E. Atkins, "Elements of X-ray Diffraction," *Physics Bulletin*, vol. 29, no. 12, pp. 572–572, Dec. 1978, doi: 10.1088/0031-9112/29/12/034.

[58] C. Suryanarayana and M. G. Norton, "Lattices and Crystal Structures," in *X-Ray Diffraction*, Boston, MA: Springer US, 1998, pp. 21–62. doi: 10.1007/978-1-4899-0148-4_2.

[59] K. D. V. Parry, "Microscopy: an introduction," vol. 13, no. 4, pp. 40–44, 2000.

[60] W. Zhou, R. Apkarian, Z. L. Wang, and D. Joy, "Fundamentals of scanning electron microscopy (SEM)," *Scanning Microscopy for Nanotechnology: Techniques and Applications*, pp. 1–40, 2007, doi: 10.1007/978-0-387-39620-0_1.

[61] Q. Wei, F. Huang, and Y. Cai, "Textile surface characterization methods," in *Surface Modification of Textiles*, Elsevier Inc., 2009, pp. 26–57. doi: 10.1533/9781845696689.26.

[62] A. Fadlelmoula, D. Pinho, V. H. Carvalho, S. O. Catarino, and G. Minas, "Fourier Transform Infrared (FTIR) Spectroscopy to Analyse Human Blood over the Last 20 Years: A Review towards Lab-on-a-Chip Devices," *Micromachines*, vol. 13, no. 2. MDPI, Feb. 01, 2022. doi: 10.3390/mi13020187.

[63] C. N. Lunardi, A. J. Gomes, F. S. Rocha, J. De Tommaso, and G. S. Patience, "Experimental methods in chemical engineering: Zeta potential," *Canadian Journal of Chemical Engineering*, vol. 99, no. 3. Wiley-Liss Inc., pp. 627–639, Mar. 01, 2021. doi: 10.1002/cjce.23914.

[64] B. R. Kirupakar, B. A. Vishwanath, M. Padma Sree, and Deenadayalan, "Vibrating Sample Magnetometer and Its Application In Characterisation Of Magnetic Property Of The Anti Cancer Drug Magnetic Microspheres," *International Journal of Pharmaceutics & Drug Analysis*, vol. 4, no. 5, pp. 227–233, 2016, Accessed: Jun. 14, 2024. [Online]. Available: http://ijpda.com;

[65] D. L. Huber, "Synthesis, properties, and applications of iron nanoparticles," *Small*, vol. 1, no. 5. pp. 482–501, May 2005. doi: 10.1002/smll.200500006.

[66] S. M. Taghizadeh, A. Berenjian, M. Zare, and A. Ebrahiminezhad, "New perspectives on iron-based nanostructures," *Processes*, vol. 8, no. 9. MDPI AG, Sep. 01, 2020. doi: 10.3390/PR8091128.

[67] W. Wu, C. Z. Jiang, and V. A. L. Roy, "Designed synthesis and surface engineering strategies of magnetic iron oxide nanoparticles for biomedical applications," *Nanoscale*, vol. 8, no. 47, pp. 19421–19474, Dec. 2016, doi: 10.1039/c6nr07542h.

[68] A. Gallo-Cordova, D. Almeida Streitwieser, M. del Puerto Morales, and J. G. Ovejero, "Magnetic Iron Oxide Colloids for Environmental Applications," in *Colloids - Types, Preparation and Applications*, IntechOpen, 2021. doi: 10.5772/intechopen.95351.

[69] P. Katikaneani, A. K. Vaddepally, N. Reddy Tippana, R. Banavath, and S. Kommu, "Phase Transformation of Iron Oxide Nanoparticles from Hematite to Maghemite in Presence of Polyethylene Glycol: Application as Corrosion Resistant Nanoparticle Paints," *Journal of Nanoscience*, vol. 2016, pp. 1–6, Aug. 2016, doi: 10.1155/2016/1328463.

[70] R. Han, W. Li, W. Pan, M. Zhu, D. Zhou, and F. S. Li, "1D magnetic materials of Fe3O4 and Fe with high performance of microwave absorption fabricated by electrospinning method," *Sci Rep*, vol. 4, Dec. 2014, doi: 10.1038/srep07493.

[71] C. Park, J. Jung, C. W. Lee, and J. Cho, “Synthesis of Mesoporous α-Fe 2 O 3 Nanoparticles by Non-ionic Soft Template and Their Applications to Heavy Oil Upgrading,” *Sci Rep*, vol. 6, Dec. 2016, doi: 10.1038/srep39136.

[72] M. Alagiri and S. B. A. Hamid, “Green synthesis of α-Fe2O3 nanoparticles for photocatalytic application,” *Journal of Materials Science: Materials in Electronics*, vol. 25, no. 8, pp. 3572–3577, 2014, doi: 10.1007/s10854-014-2058-0.

[73] M. B. Goudjil, H. Dali, S. Zighmi, Z. Mahcene, and S. E. Bencheikh, “Photocatalytic degradation of methylene blue dye with biosynthesized Hematite α-Fe2O3 nanoparticles under UV-Irradiation,” *Desalination Water Treat*, vol. 317, Jan. 2024, doi: 10.1016/j.dwt.2024.100079.

[74] P. O. Oladoye, T. O. Ajiboye, E. O. Omotola, and O. J. Oyewola, “Methylene blue dye: Toxicity and potential elimination technology from wastewater,” *Results in Engineering*, vol. 16. Elsevier B.V., Dec. 01, 2022. doi: 10.1016/j.rineng.2022.100678.

[75] A. Ahmad *et al.*, “Recent advances in new generation dye removal technologies: Novel search for approaches to reprocess wastewater,” *RSC Advances*, vol. 5, no. 39. Royal Society of Chemistry, pp. 30801–30818, 2015. doi: 10.1039/c4ra16959j.

[76] Z. A. Che Ramli *et al.*, “Photocatalytic degradation of methylene blue under UV light irradiation on prepared carbonaceous TiO2,” *Scientific World Journal*, vol. 2014, 2014, doi: 10.1155/2014/415136.

Certificate of Workshop attended

Attended DST-PURSE sponsored offline workshop & hands-on training on “Spectroscopy, Separation, and Surface Characterization Techniques” organized by Department of Chemistry and Biochemistry, Thapar Institute of Engineering and Technology, Patiala, Punjab from 4-6 March 2024.

DST@ 1971-2021

विज्ञान एवं प्रौद्योगिकी विभाग
DEPARTMENT OF SCIENCE & TECHNOLOGY

THAPAR INSTITUTE
OF ENGINEERING & TECHNOLOGY
(Deemed to be University)

CERTIFICATE OF PARTICIPATION

This acknowledges that

URVASHI CHAWLA

from DELHI TECHNOLOGICAL UNIVERSITY

has attended DST-PURSE sponsored three-day workshop & hands-on training on *"Spectroscopy, Separation, and Surface Characterization Techniques"*, organized by Department of Chemistry and Biochemistry (DCBC), during March 04-06, 2024 at Thapar Institute of Engineering and Technology (TIET), Patiala, Punjab

Prof. Amjad Ali
Organizer of Workshop
TIET, Patiala, Punjab

Prof. Soumen Basu
Organizer of Workshop
TIET, Patiala, Punjab

Prof. Manmohan Chhiber
Head DCBC
TIETPatiala, Punjab

13% Overall Similarity

Top sources found in the following databases:

- 10% Internet database
- Crossref database
- 9% Submitted Works database
- 5% Publications database
- Crossref Posted Content database

TOP SOURCES

The sources with the highest number of matches within the submission. Overlapping sources will not be displayed.

1	**Delhi Technological University on 2024-05-01** Submitted works	<1%
2	**dspace.dtu.ac.in:8080** Internet	<1%
3	**dspace.dtu.ac.in:8080** Internet	<1%
4	**researchgate.net** Internet	<1%
5	**Florian Kraushofer, Zdenek Jakub, Magdalena Bichler, Jan Hulva et al. ...** Crossref	<1%
6	**link.springer.com** Internet	<1%
7	**pubs.rsc.org** Internet	<1%
8	**nature.com** Internet	<1%

9	Banaras Hindu University on 2024-06-06 Submitted works	<1%
10	University of Leeds on 2014-06-25 Submitted works	<1%
11	Banaras Hindu University on 2024-05-09 Submitted works	<1%
12	Tadele Assefa Aragaw, Fekadu Mazengiaw Bogale, Belete Asefa Araga... Crossref	<1%
13	Sraa Abu-Melha. "Distinguishable photocatalytic activity of nano polya... Crossref	<1%
14	Ahmadi, Shideh, Chin-Hua Chia, Sarani Zakaria, Kasra Saeedfar, and Ni... Crossref	<1%
15	Delhi Technological University on 2019-05-21 Submitted works	<1%
16	ebin.pub Internet	<1%
17	macau.uni-kiel.de Internet	<1%
18	ijsrst.com Internet	<1%
19	Curtin University of Technology on 2022-09-08 Submitted works	<1%
20	khazna.ku.ac.ae Internet	<1%

21	mdpi.com Internet	<1%
22	University of St Andrews on 2022-09-12 Submitted works	<1%
23	coek.info Internet	<1%
24	Multimedia University on 2011-11-09 Submitted works	<1%
25	ceram.com Internet	<1%
26	Adamson University on 2017-09-12 Submitted works	<1%
27	Institute of International Studies on 2022-01-04 Submitted works	<1%
28	Kuwait University on 2022-02-28 Submitted works	<1%
29	kipdf.com Internet	<1%
30	openarchive.usn.no Internet	<1%
31	tudr.thapar.edu:8080 Internet	<1%
32	vital.seals.ac.za:8080 Internet	<1%

33	rjlbpcs.com Internet	<1%
34	CSU, Dominguez Hills on 2024-05-07 Submitted works	<1%
35	Curtin University of Technology on 2024-06-02 Submitted works	<1%
36	Muhammad Farooque Lanjwani, Mustafa Tuzen, Muhammad Yar Khuh... Crossref	<1%
37	Soares, Paula Isabel Pereira. "Chitosan-Based Magnetic Nanoparticles ... Publication	<1%
38	Universiti Teknologi MARA on 2012-10-29 Submitted works	<1%
39	d.docksci.com Internet	<1%
40	hdl.handle.net Internet	<1%
41	Addis Ababa Science and Technology University on 2024-03-02 Submitted works	<1%
42	Ahmad, Akil, Siti Hamidah Mohd-Setapar, Chuo Sing Chuong, Asma Kh... Crossref	<1%
43	Delhi Technological University on 2024-03-27 Submitted works	<1%
44	addi.ehu.es Internet	<1%

45	c.coek.info Internet	<1%
46	libuwspaceprd02.uwaterloo.ca Internet	<1%
47	patents.google.com Internet	<1%
48	Khushbu Kumari, Aditya Nandi, Adrija Sinha, Pritam Kumar Panda et al.... Crossref	<1%
49	Kwame Nkrumah University of Science and Technology on 2016-08-28 Submitted works	<1%
50	Scanning Microscopy for Nanotechnology, 2007. Crossref	<1%
51	University of Leicester on 2022-03-04 Submitted works	<1%
52	VIT University on 2015-07-22 Submitted works	<1%
53	Van Lang University on 2023-07-26 Submitted works	<1%
54	bjp.sagepub.unboundmedicine.com Internet	<1%
55	krishikosh.egranth.ac.in Internet	<1%
56	pubag.nal.usda.gov Internet	<1%

57	repository.library.carleton.ca Internet	<1%
58	deswater.com Internet	<1%
59	Indian Institute of Technology on 2024-04-21 Submitted works	<1%
60	Jaypee University of Information Technology on 2017-09-22 Submitted works	<1%
61	Saveetha Dental College and Hospital, Chennai on 2023-10-09 Submitted works	<1%
62	UCSI University on 2023-08-01 Submitted works	<1%
63	University of Bristol on 2012-01-23 Submitted works	<1%
64	University of KwaZulu-Natal on 2021-04-15 Submitted works	<1%
65	University of Pune on 2014-11-29 Submitted works	<1%
66	core.ac.uk Internet	<1%
67	idr.mnit.ac.in Internet	<1%
68	microbialcellfactories.biomedcentral.com Internet	<1%